ADDIS ABABA UNIVERSITY

Addis Ababa Institute of Technology

School of Mechanical and Industrial Engineering

Analyzing The Influence of Material property of Railway Wheel Steel under High Temperature on AALRT

By

Yabetse Medalcho

A Final Report submitted to the Graduate School of Addis Ababa University

Master of Science in Mechanical Engineering

(Under Railway Engineering)

Advisor

Mr. Habtamu Tkubet (Msc.)

JUNE, 2017

ADDIS ABABA UNIVERSITY

ADDIS ABABA INSTITUTE OF TECHNOLOGY

SCHOOL OF MECHANICAL AND INDUSTRIAL ENGINEERING

Master's Program Final Thesis Acceptance Approval Form

Thesis Title: Analyzing The Influence of Material Property of Railway Wheel Steel Under Thermo-mechanical Stress on AALRT

By : Yabetse Medalcho

July, 2017

APPROVED BY BOARD OF EXAMINERS

_____	_____	_____
Railway Center Head	Signature	Date
_____	_____	_____
Advisor	Signature	Date
_____	_____	_____
Internal Examiner	Signature	Date
_____	_____	_____
External Examiner	Signature	Date

DECLARATION

I hereby declare that the work, which is undertaken in this thesis entitled "**Analyzing The Influence of Material Property of Railway Wheel Steel Under Thermo-mechanical Stress on AALRT"** is original of my own, one of the problems AALRT is currently facing and has not been presented for a degree of any other university and all the resource materials used for this work have been currently referred.

_____ _____

Yabetse Medalcho Date

This is to certify that the above declared made by the candidate is correct to the best of my knowledge.

_____ _____

Mr. Habtamu Tkubet

(Advisor) Date

Acknowledgment

First and foremost I would like to praise the Almighty God who helps me in my entire journey. Next I would like to thank my advisor Mr. Habtamu Tkubet, for his continuous support and follow up. I also want to express my gratitude to AAIT staff Mr. Nathnael who helped me on ABAQUS software, Mr. Tsegaye F. and M. Tollosa D. for their continuous follow up and comments to finalize my paper and all ERC staffs who assisted me to find relevant data from the corporation.

Abstract

During the train emergency brake phenomenon, wheel locking takes place due to a high braking force applied on the wheel that exceeds the traction force between the wheel and rail. A wheel locking is a phenomenon in which the wheel stops rolling over the rail and exhibits skidding of a wheel on rail. This skidding motion of the wheel induces a rise in temperature on the wheel and rail surface. In some cases, this rise in temperature tends to change the microstructure of the wheel surface leading to the reduction of wheel strength and plastic deformation. Addis Ababa Light Rail Transit (AALRT) maintenance workshop executes the re-profile of the wheel when defects like plastic deformation, spall, and wear are encountered. In the meantime, continues re-profiling of rail wheels shortens the wheel life resulting in an increase in the maintenance cost of the company.

This paper presents the mechanical property comparison of two railway wheel plates of steel with different chemical compositions. This study is carried out on UIC passenger train wheels. UIC puts a standard of wheel grade with different alloying percentages for different train applications. For this specific research two passenger wheel classes such as R6T and R8T are selected for comparison. By varying the alloying percentage of wheel steel, the variation in the mechanical and thermal property of the wheel is studied for the train emergency brake phenomenon which exhibits skidding for most of the cases. FEA software is used as a method of research to analyze the phenomenon. By increasing the alloying percentage of Silicon and Manganese the Thermal and Mechanical property of the wheel is maintained in large. Manganese increases hardness and wears resistance by increasing toughness and work hardening while Silicon plays the primary role in improving thermal stability and high-temperature strength and Chromium increases corrosion resistance. The study result complies that the specific elements alloying percentage can enhance the mechanical and thermal property by improving Solid-solution strengthening of the wheel and can reduce the plastic deformation that could be induced during emergency braking and wheel skidding phenomenon. The research outcome can help the company, AALRT to employ the proper wheel material in operation and reducing the maintenance and operational cost that could be incurred due to wheel re-profile.

Keywords - Temperature Rise, Solid-solution strengthening, Silicon, Skidding, Re-profile

Table of Content

List of figures

List of Tables

Acronyms

UIC : International Union of Railways

WEL : White etching layer

AALRT : Addis Ababa Light Rail Transit

RCF : Rolling Contact Fatigue

HiSi : High silicon manganese alloy wheel steel

SEM : scanning electron microscopy

Outline of the research

This research is aim to conduct a software simulation on three UIC standard passenger wheels that are used for light weight application. The simulation involves mechanical and thermal loading analysis to obtain the plastic deformation of the two wheel materials during rolling phenomenon. In order to obtain this result the research is organized in the following chapters.

Chapter One-Introduction: The introduction section begins with introducing railway wheel structure and their operating requirements. It continues by introducing about phase change phenomenon on railway wheels. It also discusses about phenomenon observed on wheel steel during train operation. Finally the introduction section ends by discussing the major damages on wheel and the major causes of wheel damage.

Chapter Two-Literature review: This part of the research entails on discussion of different journals and articles that are done by different scholars in different countries. The chapter is divided in to three sub topics. The first subtopic reviews journals that are written on temperature and phase transformation of wheels. The influence of alloying element inhibiting on plastic deformation is discussed in the second subtopic of this chapter. The chapter also correlates chemical composition and temperature.

Chapter Three-Analytical method to analyze plastic deformation and temperature rise: In this section of the research different analytical formulas and theories that are relevant to analyze the phenomena are discussed. The theories and analytical formulas depict about wheel rail contact dynamics, thermal load on wheel and plastic deformation. It consists of derivation of different formulas that are helpful to calculate input data for the simulation.

Chapter Four-Modeling and Analysis: This part involves modeling of wheel and rail using a software ABAQUS and analyzing the models using the required parameters.

Chapter Five-Result and Discussion: The results from the software simulations are described graphically and using figures. The graphs and figures are compared and discussed for two materials.

Chapter six-Conclusion, Recommendation and Future work: Here in this chapter conclusion is drawn from the obtained results and the discussion in the previous chapter

CHAPTER 1: INTRODUCTION

1.1. Background

1.1.1. Structure and characteristics of railway wheel

A railway wheel, together with an axle, is one of the crucial parts that support the safe operation of railway vehicles. Wheels support the entire weight of cars; however, they cannot be designed as a failsafe structure where a backup system by other parts can be applied in case of a serious problem. Therefore, absolutely high reliability is demanded in terms of strength. Accordingly, the most important and fundamental characteristic in designing wheels is strength [30].

However, since "being unbreakable" is a significant wheel characteristic, from the viewpoint of advantageous performance, characteristics other than strength, such as wear resistance, thermal crack resistance, and noise/vibration, are often focused. In particular, since wheels are expendable parts, their life plays a significant role in saving the maintenance cost [29-30].

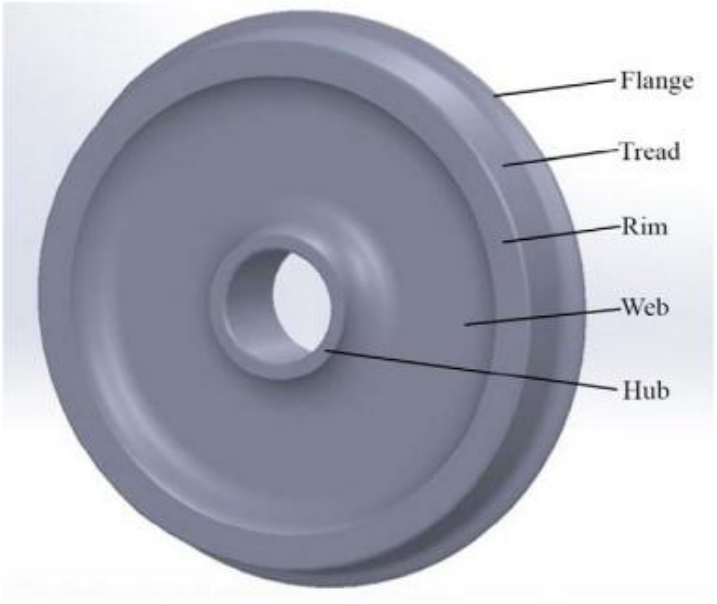

Figure 1.1. Structure of railway wheel [30]

A solid wheel of a railway vehicle consists of three parts, as shown in fig 1.1. They include a hub, where an axle is inserted, a rim that contacts the rail, and a web that unites the two parts. The outer circumferential surface of the rim, which contacts the rail, is tread, and the projected part is flange [30]. In order to achive the requiered operational performance, a railway wheel should aquire the following characterstics.

Following are the characteristics required for wheels:

1. **Weight**: Wheels are unsprang parts; therefore lightweight is preferable from the viewpoints of their influence over riding comfort and bogie parts. This characteristic is especially important when designing high-speed vehicles [30].
2. **Web fatigue strength**: A web must have sufficient fatigue strength to withstand cyclic mechanical stress caused by the weight of the car body [30].
3. **Rolling contact fatigue strength of tread**: Sufficient fatigue strength to withstand the rolling contact stress (Hertz stress) between the tread and rail is necessary [30].
4. **Characteristics of stress alternation caused by thermal attach**: When a rim expands because of thermal input caused by tread braking, thermal stress is developed at the web and rim areas. Sometimes the excessive thermal input changes the normal stress distribution given by the production stage into an abnormal situation [30].
5. **Thermal crack and fracture resistance**: This is the characteristic relating to thermal cracks initiated on a rim by the frictional heat generated by tread brake and their propagation. In worst case, wheel fracture takes place [30].
6. **Wear resistance**: Abrasion/wear is developed on a tread when it is in contact with a rail. In case of a tread brake wheel, it is also developed by the friction between brake shoes and the tread. This is the characteristic directly related to wheel life. In some cases, nonuniform wear becomes problematic rather than the wear amount itself [30].
7. **Running performance**: Running stability on a straight track and curving performance are to be evaluated basically from the viewpoint of the whole performance of a bogie. However, the tread profile is one of those factors [30].
8. **Acoustic characteristics**: Reduction of wheel running noise is required from the viewpoint of environmental demand. There are several approaches such as improvement of bogie structure or

oil lubrication on rails. As for the countermeasures taken for wheels, noise dumping wheels fitted with sound absorbers are generally employed.

9. **Vibration**: Vibration caused by a wheel is basically classified as the one caused by damages on a tread and the other caused by imbalance of a wheel. The former is influenced by the Above mentioned rolling contact fatigue strength and the wear resistance of the tread. The latter, balance characteristic, generally depends on the machining accuracies at manufacture and/or maintenance. Thischaracteristic is important for wheels of high-speed vehicles in particular.

(10) **Axle gripping force:** This is a characteristic to fix a wheel onto an axle firmly. However, there is no problem in general when interference and press-fitting force are properly controlled as per regulations [30].

1.1.2. Phase change phenomenon in wheel steel

Based on the arrangement of phases and the type of phase present, a metal can have different type of microstructure. Spherodite, Pearlite, Bainite and Martensite are among the major metal microstructures.

Phase transformation is an alteration of metal microstructure and arrangement in order to achieve a desired mechanical property. The progress of a phase transformation may be broken down into two distinct stages: nucleation and growth. Nucleation involves the appearance of very small particles, or nuclei of the new phase (often consisting of only a few hundred atoms), which are capable of growing. During the growth stage these nuclei increase in size, which results in the disappearance of some (or all) of the parent phase. The transformation reaches completion if the growth of these new phase particles is allowed to proceed until the equilibrium fraction is attained [40].

Morphology and formation of pearlite

Pearlite is a two-phase structure formed during the transformation from austenite. It grows from nuclei that exist in the prior austenite grain boundaries [39]. These nodules grow until they finally meet with each other. Pearlite colonies that consist of alternating lamellas of ferrite and cementite (Fe3C) exist within each nodule and have a single orientation. In steels with hypo-eutectoid composition, free ferrite is also present in the microstructure [39].

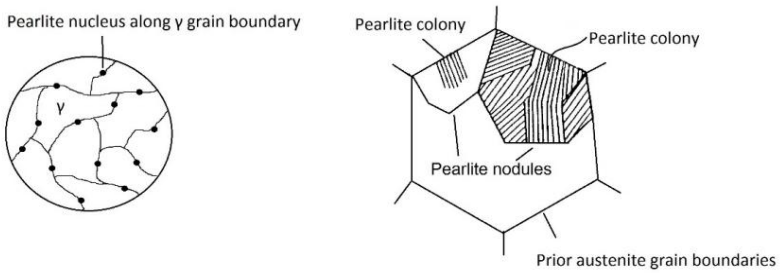

Figure 1.2. Pearlite formation [39]

The transformation temperature determines the resulting inter lamellar spacing, controlled by the carbon diffusion rate. Thus, it can be manipulated using specific heat treatments depending on the chemical composition of the material. Heat treatments that employ rapid cooling have the ability to delay the transformation temperature to lower temperatures, which in turn results in larger volume fraction of pearlite (with slightly hypo-eutectoid composition) and a refined lamellar structure [39].

Martensite formation

The notation martensite in metallurgy generally stands for diffusion less processes where all transforming atoms are displaced simultaneously [14]. Alternation of the crystal lattices results in a global dimensional change with increased volume, often associated with internal strains and risk of cracking. The iron-carbon martensite structure is unstable and already for moderate heating will start to decompose into more stable phases. Martensite is a hard and brittle microstructure that forms when the material is elevated above the austenitization temperature of the material and followed by rapid cooling of the heated surface. A railway wheel is always prone to the formation of martensite due to its operation under high thermal stress.

1.1.3. Basic phenomenon observed during train operation

A train operates under sever operating condition that causes temperature rise, plastic deformation, spalling and wear on the wheel. During the operation of trains, high thermal loads are evolved because of frictional heating on recurring acceleration, braking, curving and occasional full slippage [9].

1.1.3.1. Temperature rise

During the operation of train, the temperature of the wheel raises tremendously that causes material property change and deterioration. As the wheel–rail slip, the temperature is high enough to austenitise the material close to the contact surface. The material is rapidly cooled by heat conduction into the rest of the wheel when the wheel set starts rolling again. The cooling will be very efficient by heat conduction into the cold wheel material. The rapid temperature increase followed by rapid cooling cause's martensite to form close to the surface. In this transformed layer, cracks are often formed which can propagate into the wheel during service. This can lead to spalling, which means that pieces of the material fall off or, in the worst case, fracture of the entire wheel. To minimise damage on train and track and to avoid risk for accidents to occur, the wheels have to be machined or replaced as soon as possible to get rid of all transformed volumes and cracks. Wheel replacement and turning cause large extra costs [5]. This repeated variation in temperature causes a wheel flattening and crack formation that leads to spalling and wear. This thermal deterioration of railway wheel is detrimental to bearings and tracks. Wheel flats can also affect safety, riding comfort and noise emission [5].

1.1.3.2. Plastic deformation

Wheel flattening: It is one of the major plastic deformations caused by the intense friction between wheel and rail. Intense friction is related to wheel/rail slippage, which is local wheel material alteration with possible material detachment if defects become serious [42].

Figure 1.1.3. Wheel flattening [42]

Indentation: This damage phenomenon is due to the presence of small external object at wheel/rail interface on the track causing little indentation on the wheel rolling surface [42].

Figure 1.4. Wheel indentation [42]

Rolling contact fatigue (RCF) : As a wheel undergoes the hunting motion there is a significant value of irregularities on the wheel/rail interface. Because of the wheel – rail contact irregular network, crack or layered metal flake is generated on the entire circumference of the wheel thread. This crack and metals flakes leads the wheel into rolling contact fatigue [42].

Figure 1.5. Wheel rolling contact fatigue [42]

Spalling: It is a well-known rolling contact fatigue (RCF) damage for the railway wheel. During a wheel-rail slide caused by excessive braking or acceleration, the friction heat is sufficient enough to austenitize the material near the contact surface. Then the material is rapidly cooled by heat conduct into the adjacent material and thus the white etching layer (WEL) forms on the wheel tread [1–4]. Besides, impact loading would be generated since the wheel tread is disrupted during the wheel-rail slide. Cracks often initiate in the WEL and then propagate into the wheel due to cyclic rolling contact. The cracked material may break away from the railway wheel, leaving voids known as spall [6].

The spalling of railway wheel includes two stages, WEL formation occurring above austenitization temperature and rolling contact fatigue cracking within the material containing WEL.

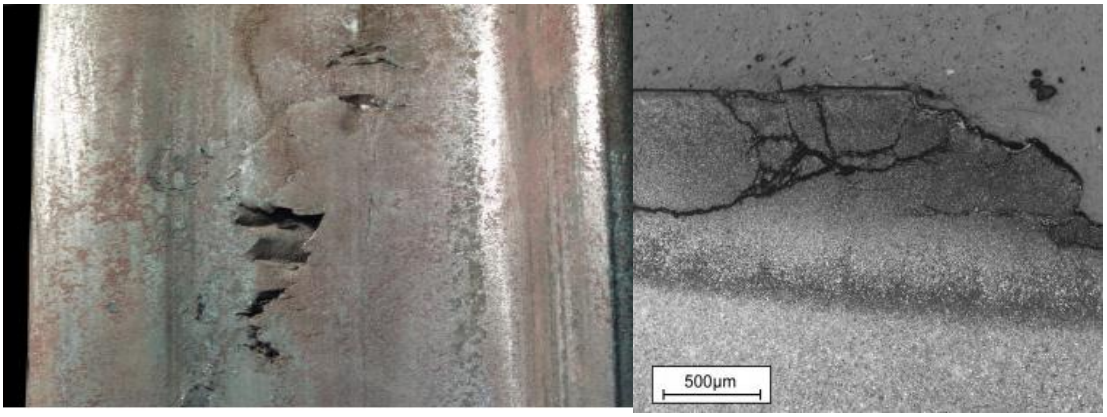

Figure 1.6. Spalling of wheel [6]

1.1.4. Factors that cause wheel steel deformation

The most important parameters that influence material transformation during railway wheel skidding are the following. Firstly, the *material_characteristics* are very important; especially the transformation kinetics is strongly dependent on chemical composition, grain size and initial phase distribution. Secondly, the *axle_load* is significant. The higher the load, the more generated heat and deformation and higher the wear rate. The *train_speed* is a third factor. It influences mainly the amount of generated heat, the wear rate and the distribution of temperatures. Fourthly, climate and contamination as well as the above mentioned factors affect the *friction coefficient*. It plays a decisive role as it, in combination with other mentioned effects, determines if slide is going to take place at all and if it occurs, it influences the heat generation. The fifth and last factor to be considered especially is the time that the wheel skids, *the locking time*. The shorter the locking time, the larger the temperature gradient, and thus the faster the cooling when the wheel starts rolling again.

1.1.4.1. Wheel steel chemical composition and its influence on wear

Carbon

Carbon controls the overall microstructure strength and hardness. It is the single most important alloying element. Increasing the carbon content rises solid solution strengthening and increases the proportion of pearlite and in addition improves wear property [14]. Increasing the carbon content increases the strength at the expense of fracture toughness [39].

Manganese

Manganese binds and helps to control Sulphur which otherwise has an embrittlement effect on the steel. In similarity to carbon, manganese increases hardness and wear resistance by refinement of pearlite lamella and is often used to compensate for a decreased carbon content. Manganese enables in solid-solution strengthening and is weak carbide former.

The eutectoid reaction can occur at lower carbon levels and by so the amount of pearlite is increased. Toughness and work hardening behavior is also improved which is important for maintaining strength in operation [14].

Silicon

It is ferrite stabilizer and has a small influence on material strength by solid solution hardening. Having a negligible solubility in cementite, silicon has proven to inhibit cementite growth or precipitation and stabilizes pearlite at exposure to high temperature. Thus silicon helps to

improve *thermal stability and high temperature strength*. Even though it's good in improving wear resistance, too high alloying content may have an embrittlment effect and negative influence on impact properties. Silicon in the steel making process is used as a DE oxidant to reduce oxygenand prohibits occurrence of iron oxide inclusions [6,7,9,14].

Molybdenum, Chromium and Vanadium

Improve wear resistance by formation of stable carbide and enhance strength and toughness. Chromium increases corrosion resistance and oxidation; in conjunction with molybdenum it increase hardenability and high temperature creep strength. Vanadium may be added to reduce excessive grain growth during heat treatments and thus promote a fine grained microstructure. Residual alloying elements primarily take part in controlling and optimizing the manufacturing process, improve cleanliness, grain refinement, and carbide formation. Their usage and amount may differ between different steel makers but normally they are limited and specified in discrete intervals for each wheel grade specification to avoid unexpected material behavior [14].

1.1.4.2. External factors that cause plastic deformation and wheel damage

The Influence of High Temperature

Medium carbon steels with around 0.55 wt.% carbon are commonly used for the manufacturing of forged railway wheels for light load applications because due to their combine good strength and wear properties. After forging, the wheels are heat treated to a microstructure consisting of mostly pearlite with some 5-10 vol. % pro-eutectoid ferrites just below the wheel tread .

During operation of trains, high thermal loads are evolved because of recurring acceleration, braking, curving and occasional slippage. During these train operation phenomenon, the temperature of the wheel increase tremendously causing a change in microstructure.

As the train starts to run it was under the normal ambient temperature it does not cause any microstructural change on the wheel. As the train continues running the temperature of the wheel tends to rise gradually. For the first minutes of the train journey i.e. until the temperature of the wheel reaches up to 300^0c, the hardness of the wheel rises significantly. When the temperature of the wheel becomes beyond 300^0c, the hardness of the wheel starts to drop down rapidly.

At exposure to medium temperatures, starting from around 400°C up to around 750°C, an increasing microstructural degeneration occurs. Since the initial microstructure is

predominantly pearlitic, the strength and wear properties of the material depend mainly on the interlamellar spacing of the pearlite. It is known that exposure to elevated temperatures yields spheroidisation of the pearlitic structure, which makes it softer. After the material has experienced plastic deformation, the material becomes even more prone to spheroidization of the lamellas on exposure to high temperatures .

Even higher temperatures up to approximately 1050°C can be reached on occasional slippage when the wheels skid along the rail for a short time. This causes phase transformations in the steel, often resulting in brittle martensitic patches on the wheel tread that can lead to spalling and other problems. Control of material property degradation in wheels is an important topic for guiding maintenance and ensuring safety of railways.

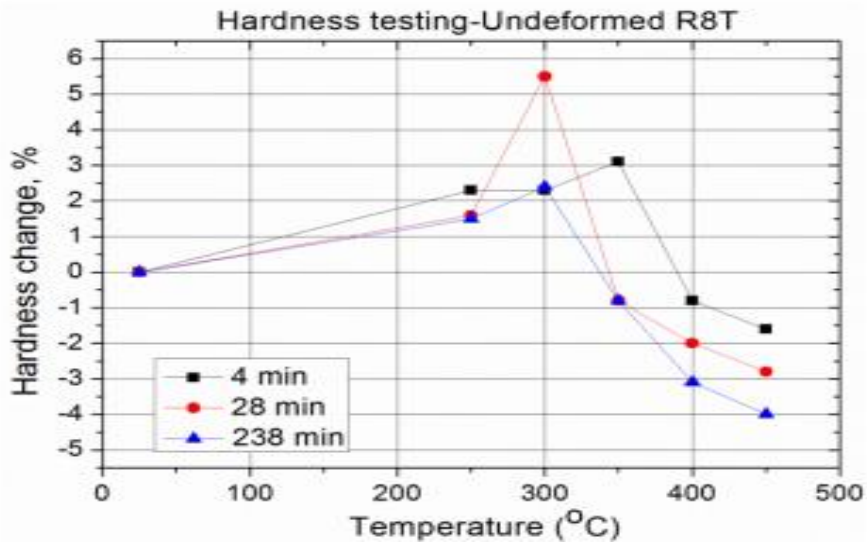

Figure 1.7. The effect of temperature rise on hardness change [9]

The effect of load

In railway traffic, the material in the contact surface of both rail and wheel undergo severe plastic deformation from vertical, tangential and longitudinal loads [11]. Non conformal contact and surface roughness may increase stresses locally in the tread surface. High contact loads initially give beneficial work hardening and compressive stresses, enhancing monotonic and cyclic performance as elastic shakedown is reached in the material. An excess of surface shear stresses may cause rolling contact fatigue (RCF) damage from accumulation of plastic strains, i.e. ratcheting [11].

- High amount of creep associated with friction and plastic deformation in the wheel rail contact from traction and dynamic loads, as when the train passes through curves or switches, can increase the temperature in the outermost tread layer. If the temperature reaches high enough, so that austenitisation takes place, martensitic phase transformation may take place upon cooling [11].

Effect of sliding

The wheel–rail slide is a very complicated tribological process. The wheel starts sliding against the rail when the frictional forces between wheel and rail cannot sustain the forces generated by the braking torque or a speed shift phenomenon. The frictional forces and the slip correspond to an evolved power P according to $p = fv$ where F is the friction force and v is the velocity [5].

The wheel slide is indeed a dynamic process. As the material close to the contacting surface gets warmer, a lot of parameters change. The Young's modulus and the yield stress decrease and the thermal diffusivity are changed. It follows that the friction coefficient cannot be treated as constant over the whole surface. Moreover, wearing causes the contact area to increase, which gradually lowers the average surface pressure. Eventually, stick–slip phenomena and thermal instability will occur between the contacting bodies [5].

1.2. Objective

1.2.1. General objective

The objective of this research is to analyze the influence of alloying elements of railway wheels on inhibiting plastic deformation and spalling at a temperature where mechanical property of wheel steel changes under a skidding phenomenon on Addis Ababa Light Rail Transit (AALRT) train.

1.2.2. Specific objective

- Modeling of wheel and rail using ABAQUS CAE software.
- Categorizing AALRT wheel steel using the UIC-standard for passenger train operation.
- Selection of two or more passenger wheel steels with different chemical composition and hardness value from the UIC wheel standard.
- Calculating the temperature rise on the wheel during wheel skidding phenomenon which usually occurs during train braking operation.
- Analyzing the thermal and mechanical loading effect using ABAQUS software for different chemical composition of wheel steel materials from the UIC standard.
- Analyzing the Thermo-dynamic stress of wheels during skidding motion and observing the plastic deformation and other damage parameters.
- Comparing the three analysed wheels using the result obtained from the finite element modeling (FEM) and finite element analysis (FEA).
- Suggesting and recommending the better wheel material based on the result and discussion.

1.3. Problem statement

A railway wheel operates under sever operating condition such as heavy load, breaking, traction and skidding. For a train operate under braking legal conditions and high loads, the severity tends to prevail. During train braking or velocity reduction, a short slippage motion known as skidding occur. During skidding (slippage) the temperature of wheel steel rises up beyond 400^0c for most of the train wheels. As the train stops this temperature drops down drastically. This repeated phenomenon creates a hard and brittle ferrous microstructure called ***martensite.*** Due to its brittleness and luck of ductility a wheel surface will be faced for plastic deformation, spalling and other wheel deteriorations.

For a Spalling length beyond $40^1/35^2$mm a corrective measure should be given based on the Maintenance Manual for Resilient Wheel of 70% Low-floor Trams of AALRT. Maintenance Manual for Resilient Wheel of 70% Low-floor Trams of AALRT show that, re-profiling is necessary when local material detachments are present along the defect length [43]. AALRT depot undergoes re-profiling on a monthly basis in order to remove wheel defects and spalling which is shortening the life of wheel. Wheel replacement and turning causes large extra costs and it's therefore crucial to find solution to the problem.

From several researches and studies on railway wheel steel, the chemical composition plays a vital role on spalling and plastic deformation of railway wheel steel. In this research, two wheel steels with different level of silicon and manganese is investigated. R6T and R8T (correspond to the UIC standard) grade wheels with different wt.% of silicon and manganese. Both grades are intended for passenger train wheel-sets and have a fine pearlitic microstructure. Applying the axle load of 11ton/axle and heat flow on the wheel surface, the wheel is subjected to a skidding phenomenon starting from the maximum speed of the train for about 1seconds. Within this short phenomenon the temperature rise and plastic deformation of the two wheels is compared. For this research a finite element modeling and analysis is carried on by the software ABAQUS. Using the software analysis the thermo-mechanical stress on the wheel will be calculated. The result of this thesis is expected to show the influence of solid-solution strengthening (alloying) in enhancing the strength and toughness of railway wheels.

1.4. Scope and Limitation and Significance of the Research

1.4.1. Scope

This research entails on analyzing the influence of material composition i.e. the effect of different alloying elements on inhibiting damage of train wheel steel as temperature rise during speed reduction and other train operations. The study involves wheel and rail modeling, selection of two passenger wheels that are used for light load application from UIC standard and finally analyzing the three wheels using FEM modeling and analysis. The analysis involves mechanical and thermal simulation during skidding of wheel using AALRT design and operation parameters. The study is limited on comparison and suggestion of better material based on the results that is obtained from finite element analysis. The analytical study entails on material selection and analyzing plastic deformation of different alloy steels and comparison based on graphs and results obtained.

1.4.2. Limitation

From several studies carried out in different countries, wheel damage prominently depends on material property and chemical composition. Most of the journals and researches in this area are carried on by material tests since the area needs extensive experimental testing and microstructural observations Mechanical test such as fatigue test and hardness test, chemical composition tests using EDS spectroscopy machine and microstructural observation using SEM (scanning electron microscopy) are among the major tests in the field of study. Due to the time limit and lack of facility this research is limited to analytical study only.

During train operation the basic heat transfer techniques such as conduction, convection and radiation takes place. But due to analysis complexity only conduction heat transfer is considered between the wheel and rail.

1.4.3. Significance of the research

- Identifying the better material that can resist plastic deformation and spalling under the current operation parameters of AALRT train.
- Bench mark for future works on wear and fatigue damage.

1.5. Methodology of the Research

This research involves the basic research methodology steps and techniques in order to achieve the desired objective. It involves;

1. Literature review on railway wheel material and properties related to deformation and damage under high temperature.

In this research literature is solely reviewed using internet. The website Science Direct.com helps to find several free journals and articles that are done by scholars on this study area. Finally these journals categorized and studied for referring.

2. Data collection from ERC (Ethiopian Railway Corporation)

The data collected from ERC are secondary data that are collected from the rolling stock department of the company. The train and wheel technical parameters are data that are collected from the company. The other secondary data collected for this research is wheel data from UIC (International Union of Railways).

3. Wheel and rail modeling using ABAQUS.

The software ABAQUS is used for the research. The software does from modeling to final analysis procedures using several modules. The module involves several tasks that should accomplish in each step.

4. Wheel simulation for plastic deformation under high temperature using ABAQUS software.

CHAPTER 2: LITERATURE REVIEW

2.1. Temperature and phase transformation of wheel steel

Carbon steel with a pearlitic microstructure is the most commonly used material for railway wheel sets due to high strength, low cost and good wear properties. However, as a result of the two-phase microstructure, pearlite is susceptible to softening at higher temperatures caused by spheroidisation of the cementite phase. The spheroidisation can eventually be more accentuated by simultaneous plastic deformation during high temperature exposure [2].

Recently a new type of wheel grades have been introduced to the market with increased content of silicon and manganese which is assumed to be more resistant to rolling contact fatigue and thermal damage. Historically wheel steel grades have been designed to be resistant against martensite formation which makes wheel sets prone to mechanical damage. The development of modern braking systems today to a large extent has eliminated full locking of wheel sets on passenger trains and therefore decreased the risk of reaching above the austenitisation temperature (AC1) in the contact zone between wheel and rail. However spheroidised pearlite has been observed during maintenance of wheels, and twin disc tests have shown that temperatures in the range of approximately 500°C are present during normal running conditions [2]. Hence, thermal damage is still to be expected, but related to temperatures mainly below the alpha-gamma transformation temperature of iron.

A scholars from Sweden called K. Cvetkovski*, J. Ahlström and B. Karlsson from material and manufacturing department try to observe the effect of temperature on fatigue behavior and strength of steel wheel on their journal called, *Thermal Softening of fine pearlitic steel and its effect on the fatigue behavior (2010).* Beside the effect of temperature, the influence of chemical composition and plastic deformation on the spherodisation process and its consequence on the fatigue process also their primary concern. They conduct experimental investigation. The material and experimental procedure is as follow.

Two steels with different levels of silicon and manganese were investigated, the R8T wheel grade (corresponding to European ER8) defined by the EN13262 standard. And a second grade with 1 wt. % silicon and 0.95 wt.% manganese, here denoted as HiSi. Actual chemical compositions are given in Table 1. Both grades are intended for passenger train wheel sets and have a fine pearlitic-ferritic microstructure with 5 to10 vol. % free ferrite.

The material was obtained from new complete wheels and fatigue specimens were extracted close to thread in the running direction. Heat treatments were made in a tube furnace with a protective argon atmosphere to prevent decarburization, and slowly cooled (~100 °C/min) back to room temperature. The temperature was kept below AC1, which was estimated to 760°C for HiSi and 748°C for R8T material. Annealing temperatures were fixed to 500, 575, 650, 700 and 725 °C, with three annealing times at each temperature to facilitate easy comparison of resulting properties. Evaluation of material softening was made on coin like samples by Vickers hardness indentations (HV30), before and after heat treatments. A selection of samples where studied optically and by scanning electron microscopy (SEM) to determine the microstructure. Low cycle fatigue (LCF) evaluation were made for completely reversed push-pull test conditions in a servo-hydraulic Instron 8032 rig under strain control using a saw tooth wave shape with a constant strain rate of 1·10-2 s-1 [2].

Table 2.1. Weight percentage (wt. %) elements for HiSi steel and R8T steel wheel

	C	Si	Mn	Mo	Cr	Ni	S	P	V	Fe
HiSi	0.57	0.99	0.95	0.04	0.14	0.12	<0.001	0.008	<0.005	96.9
R8T	0.58	0.34	0.75	0.02	0.15	0.10	<0.001	0.010	<0.005	97.8

- The heat treatments revealed that below 500°C no softening occurs, as no change of hardness could be measured in neither of the materials below this temperature. The materials had similar hardness in their initial state, which was confirmed to be within limits of respective grade specifications. Initial hardness homogeneity within the sample group was 276 (HV30) ± 2. The test trials revealed (Fig.) that the temperature has a major effect on the material softening while soaking time is not as significant. Pronounced softening of the materials was seen to occur in the very initial part of the heat treatment,

i.e. within the first minutes. The HiSi material retains a higher hardness for all test temperatures, in particular in the range of 500 to 650°C the performance is substantially better with a decrease of less than 50% compared to that of R8T. The SEM study showed that spheroidising of cementite lamellas increased with longer treatment time and higher temperature. Carbides in the HiSi material were seen to be slightly smaller than those in R8T. However it could not be confirmed visually that the extent of spheroidisation within HiSi was significantly unlike that for the R8T material which earlier has been reported for similar alloyed steels [2].

- Yield (Rp0.2) and ultimate tensile (Rm) strengths for the two materials decrease in qualitatively the same manner upon annealing as do the hardness values. At the same time the ductility increases with progressed softening of the materials, but less so for HiSi. There is positive strain rate sensitivity for both materials, and this rate dependence seems rather independent of the degree of softening [2].

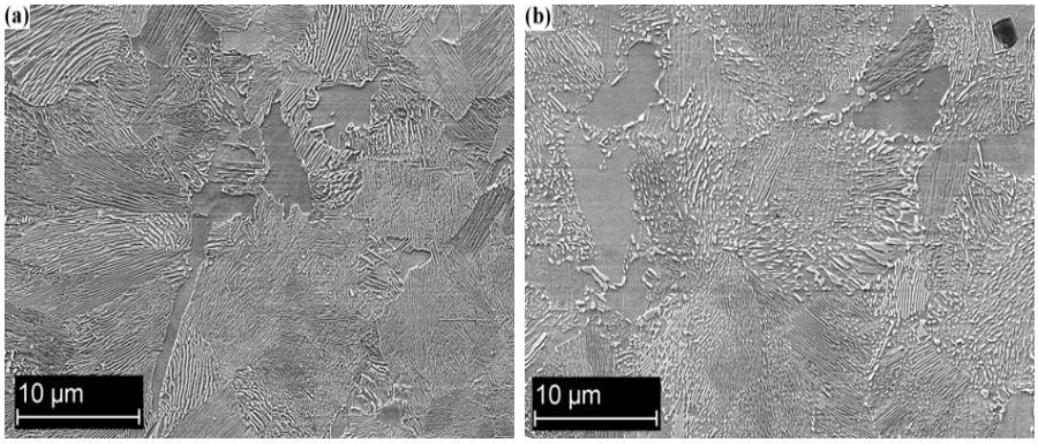

Figure 2.1. SEM micrographs, dark etching phase pro-eutectoid ferrite and mixed grey constituent pearlite. Spheroidised cementite lamellas are visible as discontinued globular carbide streaks within pearlite nodules in the heat treated state. (a) R8T, intial state and (b) R8T, heat treated (28min at 700°C).

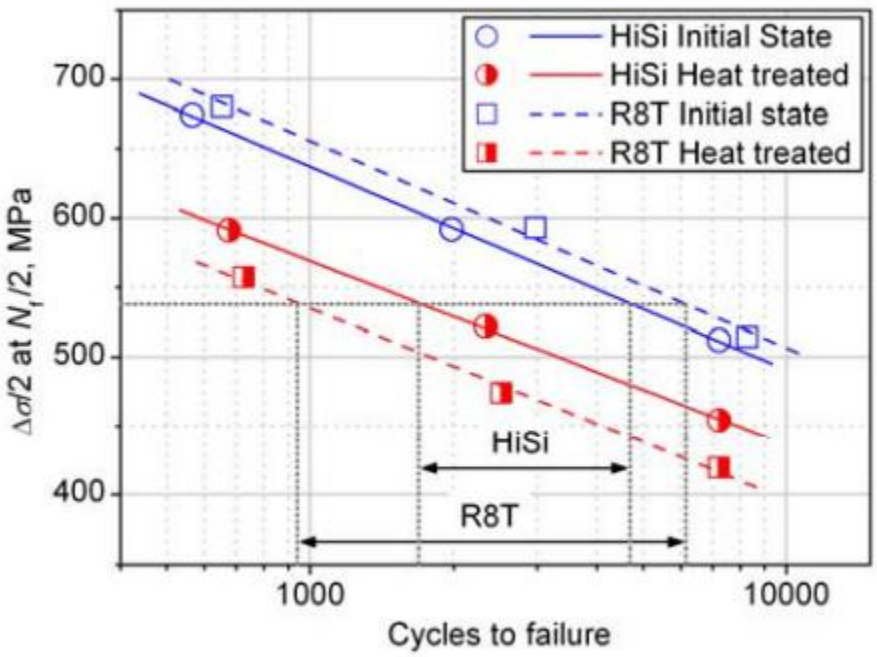

Figure 2.1. Fitted Wöhler curves demonstrate decrease of fatigue life caused by heat treatment (28 min at 700°C). Fatigue life time Nf decrease a factor two less for HiSi steel at all stress amplitudes.

- The two scholars from their experimental investigation on two wheel steels standard carbon steel (R8T) and high silicon/manganese grade (HiSi) conclude that tensile properties altered due to annealing on hardness above 500^0c. The softening is markedly less for HiSi revealing itself in reduced lowering of hardness, monotonic and cyclic yield stresses and fatigue life time [2].
- The two scholars in their work show the remarked reduction in hardness of the two wheel steels with different chemical composition. Beside the reduction of hardness due to temperature rise the formation of martensite which leads to plastic deformation and spalling due to the slippage between wheel and rail under skidding phenomenon is the research gap in their work.

The journal of another scholars from Sweden with a title *Mechanical properties and fatigue behavior of railway wheel steel as influenced by mechanical loading* [9] shows that thermal loading have high influence on microstructural degradation and reduction in hardness.

- Light optical microscopy (OM) and scanning electron microscopy (SEM) were used to evaluate the initial and final microstructures [9]. The initial microstructure consists of pearlite (dark areas) and some pro-eutectoid ferrite (brighter areas). The SEM investigation also shows that the spacing is finer close to the surface of the wheel [9].

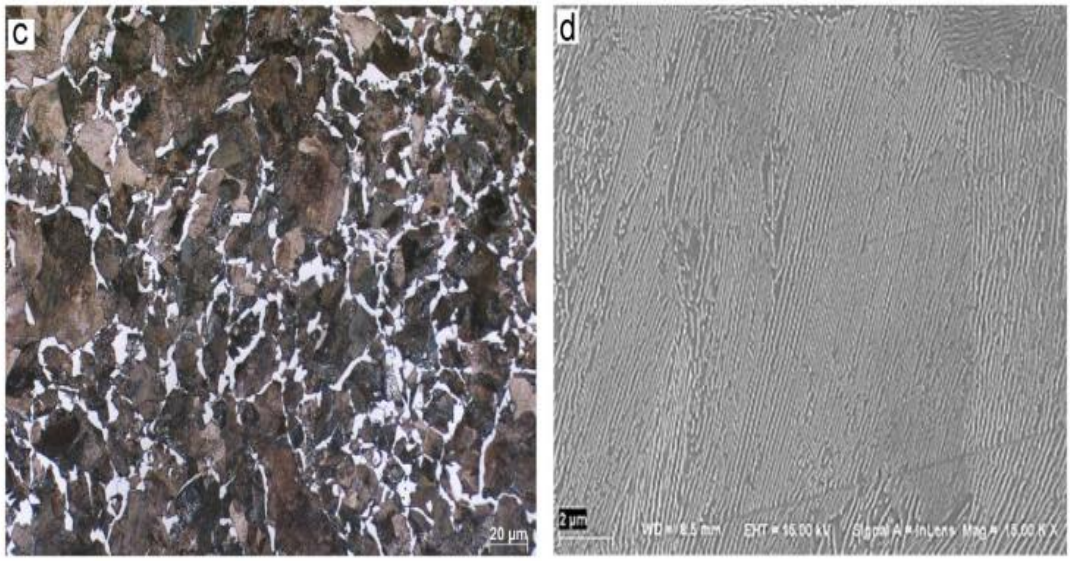

Figure 2.2. Microstructural overview of the undeformed R8T using optical microscopy and scanning electron microscopy (SEM) [9]

- The micrograph observation of their experiment reveals that the combined influence of plastic deformation and thermal exposure accelerates degradation of the microstructure. The experimental result also shows that the temperature rise also reduces the hardness of the material. At the higher temperature values 500^0c – 600^0c, the material exhibits considerably higher peak stresses and cyclically softens during the life as a result of combined thermal softening and microstructural degradation [9].

- The SEM investigation of undeformed material after the annealing treatment showed that the pearlite lamellas starts to break up around 450^0c [6-9]. This effect becomes more pronounced when the material was held at that temperature for 238mins [9].

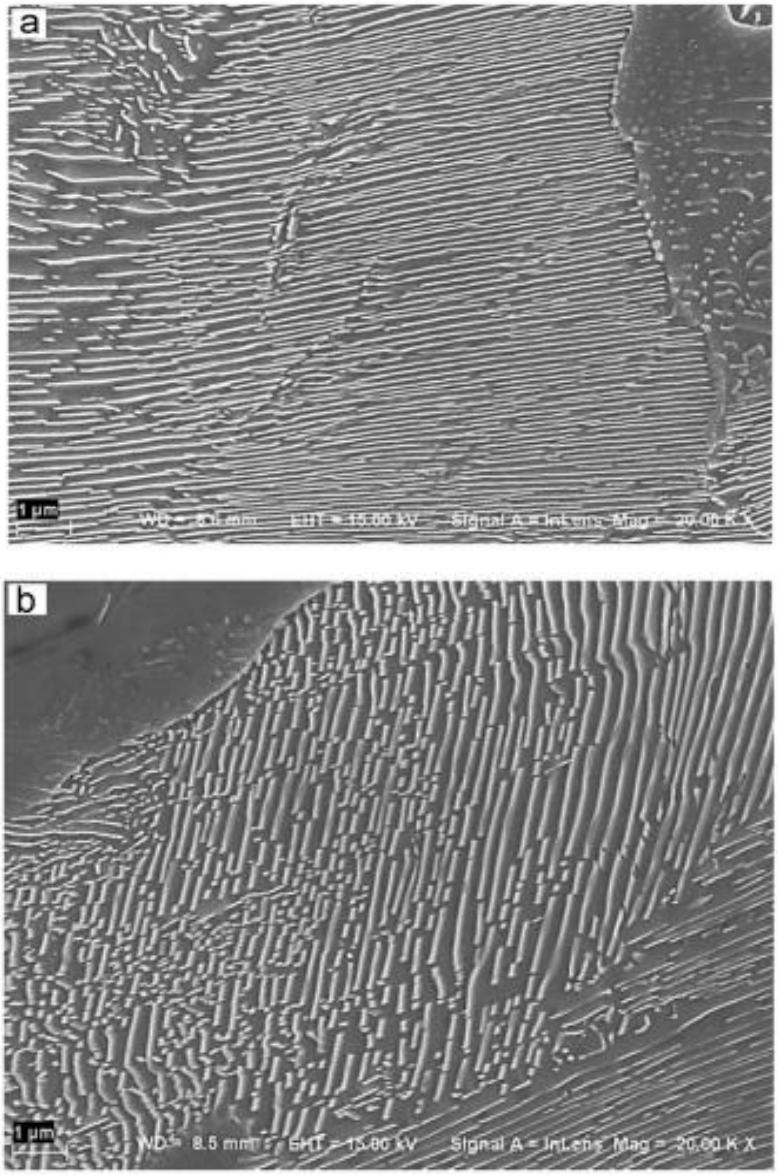

Figure 2.3. SEM micrographs of the undeformed R8T at 450°C for 28 min (a) and 238 min (b) [9].

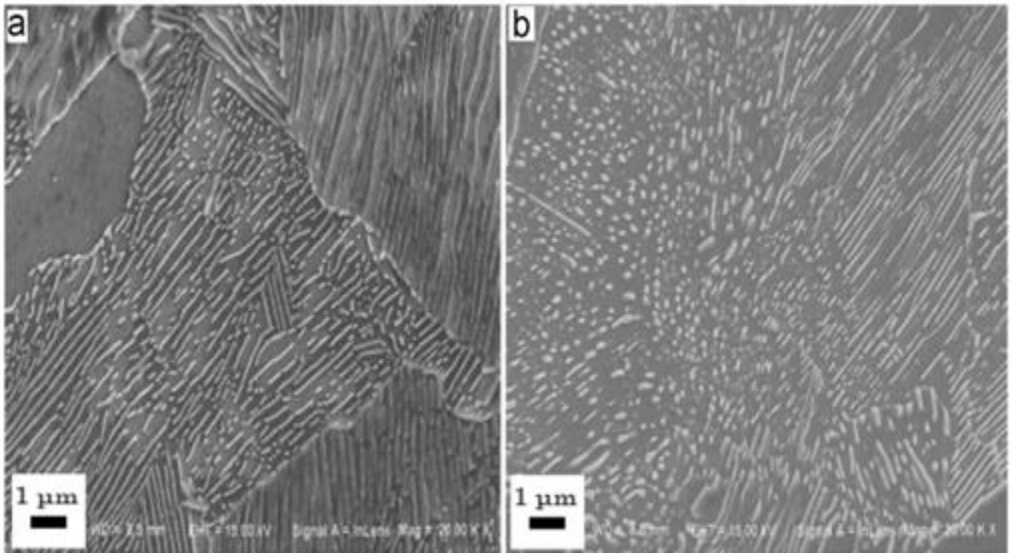

Figure 2.4. SEM micrographs of the monotonically strained R8T at 400°C (a), 500°C (b), 600°C for 28 min hold time [9]

- From their work one can conclude that higher temperature and longer time allow for stronger spherodisation which leads to the increasing drop in hardness [2,3,8,9,11,12].

2.2. Chemical Composition of Wheel and its influence on inhibiting plastic deformation

One of the remedy to overcome the rolling contact fatigue damage on wheel steel is solid solution strengthening [6]. The study of Dongfang Zeng, Liantao Lu, Yanhua Gong, Yuanbin Zhang, and Jiwang Zhang shows that rolling contact fatigue (RCF) is the detrimental factor on wheel steel that cause crack growth and spalling at the end. Spalling of railway wheel includes two stages that are *formation of white etching layer (WEL) that occur above austenitization temperature* and *rolling contact fatigue cracking within the material containing WEL* [6]. Their work with a title *Influence of solid solution strengthening on spalling behavior of railway wheel steel* includes micrographic observation for the formation of WEL and Finite Element Modeling (FEM) for analyzing the influence of rolling contact fatigue(RCF).

On their work they propose two effective methods to improve the spalling resistance of railway wheel steel which are increasing the resistance to WEL formation that primarily depends on *chemical composition (alloy design)* and delaying the RCF failure for wheel steel containing WEL.

The strength of railway wheel steel is usually increased by increasing carbon content. However, carbon addition would increase the thermal sensitivity since it reduces the austenitization temperature. This may decreases the spalling resistance of wheel steel [6]. In contrary the addition of Silicon and Manganese improves the strength of wheel steel thorough solid solution strengthening by stabilizing steel at elevated temperature and lowering thermal degradation below austenitization temperature [6].

On their work they try to compare the traditional (commercial) wheel steel (ER8) with a recently developed high silicon manganese alloy wheel steel (HiSi) to observe the influence of chemical composition on WEL formation and spalling in general.

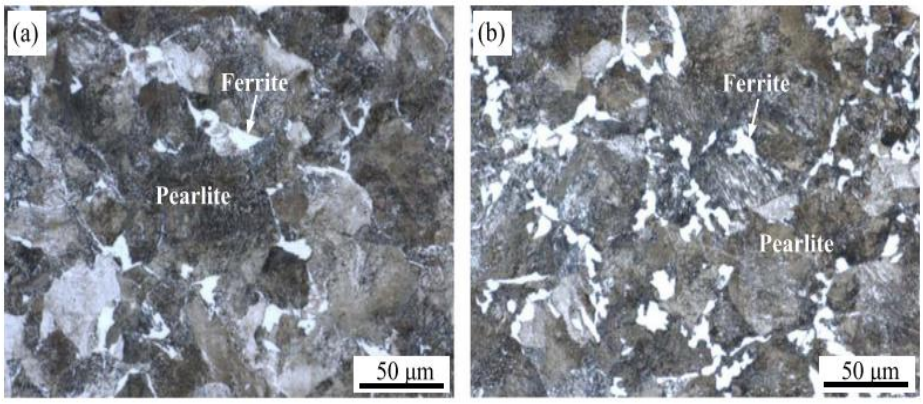

Figure 2.6. Micrographs of (a) ER8 steel and (b) HiSi steel [6].

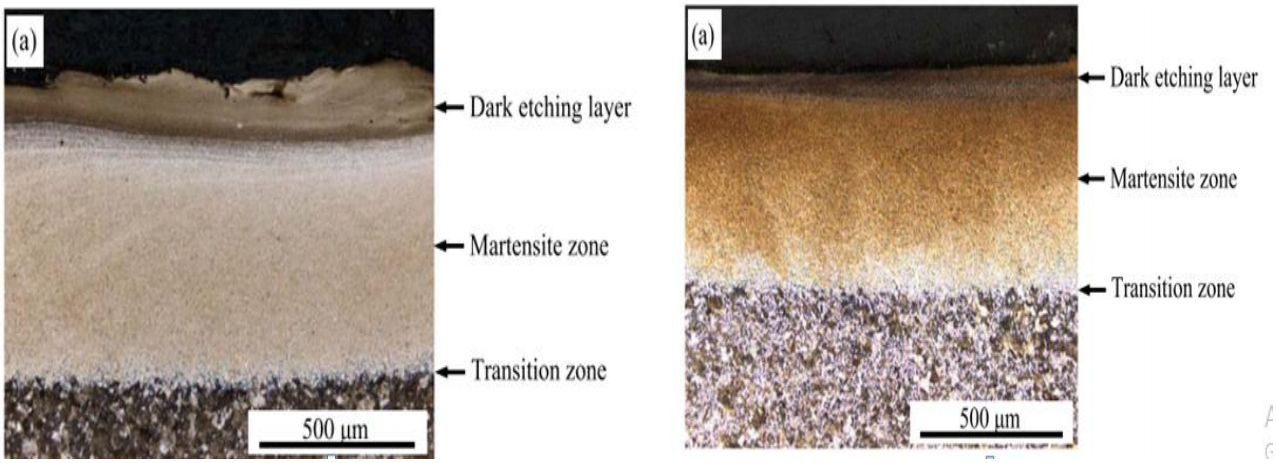

Figure 2.7. Microstructure of WEL for ER8 steel (Micrographic observation) [6] left, Microstructure of WEL for HiSi steel (Micrographic observation) [6] right

From the figure one can see that the transition zone for ER8 material is shorter compared with the recently improved wheel steel (HiSi).

Table 2.2. Size of white etching layer/μm [6].

Rank	1	2	3	4	5	6	Average
ER8	602	610	621	676	724	732	661 ± 58
HiSi	440	445	478	490	498	553	484 ± 41

As compared with ER8 steel, A1 and A3 points (*lines denoted by A1 and A3 have great effect on the progress of phase transformation. Discussed in chapter 1*) for HiSi steel only increase by 3°C and 12°C, respectively. It is likely that the improvement of resistance to WEL formation can be attributed to some other factors. It is reported that the material characteristics, including chemical composition, grain size, deformation state and initial phase distribution, are associated with the material transformation [5-6].

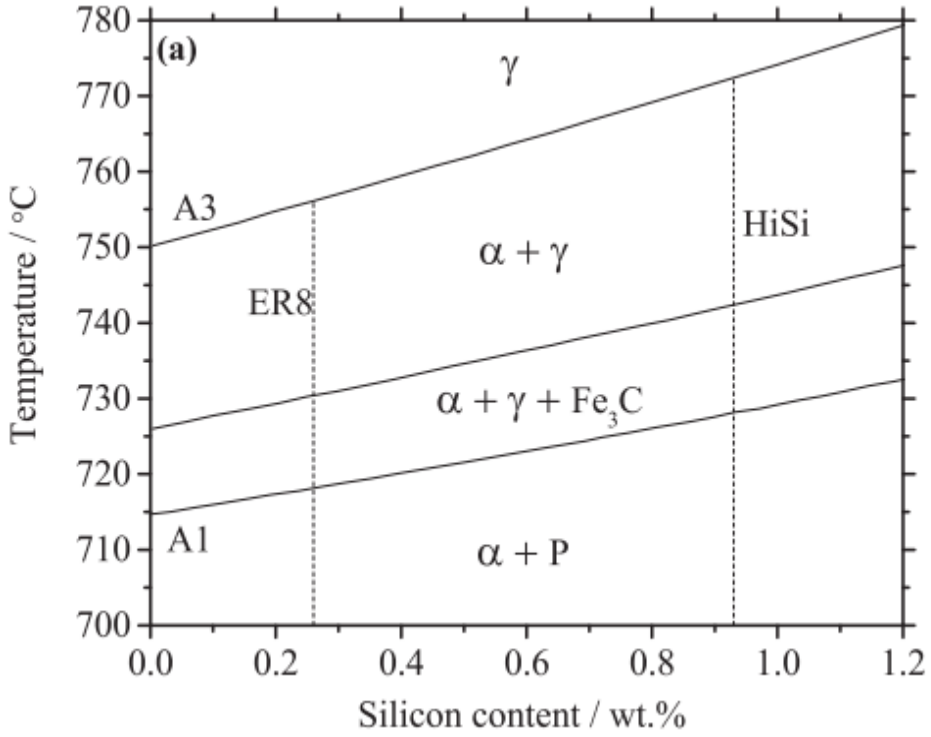

Figure 2.8.. Equilibrium phase diagram of 0.52C-(0–1.2) Si

From the micrographic observation of the two steel wheels, the following conclusions have been made.

- Silicon addition improves the resistance to WEL formation for HiSi steel wheel through increasing austenisitation temperature [5-6].
- In comparison of ER8 steel, the grain boundary density along the direction of plastic deformation is increased within HiSi steel containing WEL which tends to increase the crack growth life of WEL-HiSi [5-6].
- WEL remarkably reduced reduce the RCF life of railway wheel steel [6].

Despite their astonishing work on solid solution strengthening to overcome rolling contact fatigue (RCF), its influence on spalling behavior of railway wheel which includes WEL formation occurring above austenitization temperature and RCF behavior of steel containing WEL is still the research gap.

The other astonishing research that has done on the influence of material composition on fatigue damage of wheel steel is the Chines journal with a title *Frictional Heat-Induced Phase Transformation on Train Wheel Surface* [12].

The study tries to correlate the effect of carbon content on the martensit layer formation as the temperature rise beyond the austenitising temperature.

Many researches showed that the thermal fatigue of wheel tread was related to the formation of the martensite phase [12]. When the brakes were applied on a train, the temperature of the wheel/track contact zone increased sharply because of sliding friction. Sometimes the temperature was even higher than the phase transformation point of the wheel steel, and caused partial and even complete austenization in the wheel tread surface. When the sliding process was complete, the heated surface rapidly Cooled down because of the cold track and wheel rim, which formed a thin martensite (or mixture of phases) layer. Martensite is a hard and brittle phase, which easily resulted in cracking under cycling load [2-12].

By combining thermo mechanical coupling finite element analysis with the characteristics of phase transformation [continuous cooling transformation (CCT) curve], the thermal fatigue behavior of train wheel steel under high speed and heavy load condition was discussed [12].

The result shows that the peak temperature of wheel/track friction zone could be higher than the austenitization temperature for braking. The super cooled austenite is transformed to a hard and brittle martensite layer during the following rapid cooling process, which may lead to cracking and then spalling on the wheel tread surface.

The decrease in carbon content of the train wheel steel helps inhibit the formation of martensite by increasing the austenitization temperature of the train wheel steel. When the carbon content decrease from 0.7% to 0.4% the Ac3 of the wheel steel is increased by 45^0c and the thickness of martensite layer is decreased by 30%.

2.3. Correlation between alloying elements in railway wheel steel and temperature

Railway wheel is ferrous alloy steel composed of primarily carbon and other alloying elements. The microstructure of wheel steel varies with the depth in the wheel rim. Microstructural characterizations of tested materials at depths of 20 mm and 45 mm, including volume fraction of proeutectoid ferrite, interlamellar spacing, pearlite colony size and prior austenite grain size,were measured by the use of CLSM and SEM micrographs [27].

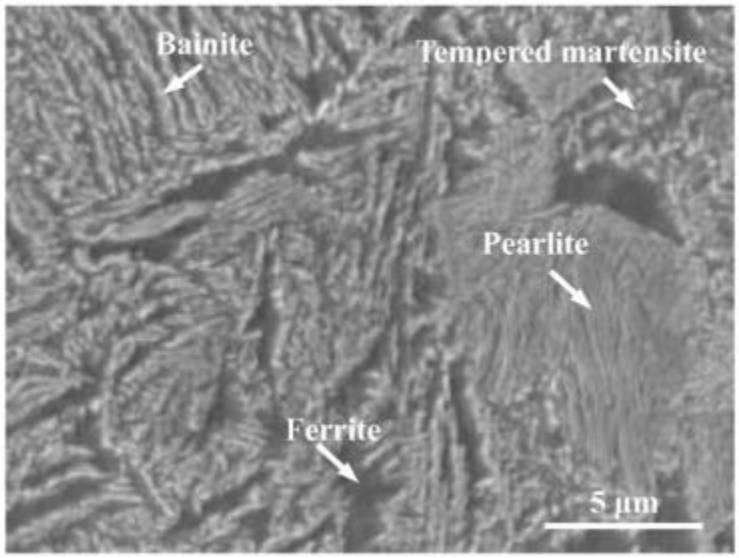

Figure 2.9.. SEM micrograph of the complex layer of ER8 wheel at a depth of 7 mm.

From several researches and studies, the microstructure of wheel falls to the pearlite microstructure. As discussed above pearlite is a hard metal layer that resists wear and plastic deformation. From the work with a title *Optimization of strength and toughness of railway wheel*

steel by alloy design [27], one can see that the formation of fine pearlite structure is dependent on alloy design and good manufacturing process.

Formation of martensite is one of the undesirable phenomenons during train operation since it has direct impact on fatigue damage, crack formation and spalling. This also can be avoided by increasing the alloying percentage and reduction of carbon content [27].

In railway wheel steel, the influence of alloying elements is observed under sever operating conditions of the train such as traction, curving and brake. From the above literatures on railway wheel steel, chemical composition plays vital role in maintaining the mechanical and thermal property of the wheel. Most of the works by different scholars is based on microstructural observation and heat treatment procedure to observe the phase change during train operation.

- Most of the studies do not consider the combined effect of temperature rise due to skidding, mechanical stress, speed reduction leading to slippage, friction and other contact mechanics parameters.
- In this research the influence of chemical composition on inhibiting plastic deformation under high temperature at the frictional surface where slippage and mechanical stress are existed analyzed using software called ABAQUS.

CHAPTER 3: ANALYTICAL METHODS FOR ANALYSING PLASTIC DEFORMATION AND TEMPERATURE RISE OF WHEEL

3.1. Wheel rail contact dynamics

Normal Contact Problem

The normal pressure at any point of the contact ellipse of two arbitrarily curved bodies is given by the Hertzian theory .

$$p(x,y) = p_0\sqrt{1-\frac{x^2}{a^2}-\frac{y^2}{b^2}} \quad \ldots\ldots\ldots\ldots (Equation\ 3.1)$$

Where a and b are the semi-axis of the contact ellipse. The magnitude of these axes depends on the radii of curvature of the contacting systems and on the normal load.

Since the maximum heat flux occurs in the z- direction, the problem can be simplified to the two dimensional contact of cylindrical bodies. The maximum pressure for the three – dimensional case is

$$p_0 = \frac{3F}{2\pi ab} \ldots\ldots\ldots\ldots\ldots (Equation\ 3.2)$$

If R_x and R_y are longitudinal and lateral and lateral relative radii of curvature respectively, then to find the size of the contact ellipse the next formula can be used:

$$\frac{A}{B} = \frac{R_X}{R_Y} = \frac{(a/b)^2 \boldsymbol{E}(e) - \boldsymbol{K}(e)}{\boldsymbol{K}(e) - \boldsymbol{E}(e)} \ldots\ldots\ldots\ldots\ldots\ldots (Equation\ 3.3)$$

$$\sqrt{AB} = \frac{1}{2}\sqrt{\frac{1}{R_x R_y}} = \frac{P_0}{G}\frac{b}{a^2 e^2}\sqrt{\left(\left(a/b\right)^2 E(e) - K(e)\right)(K(e) - K(e))} \ldots\ldots\ldots (Equation\ 3.4)$$

In which the factors K (e) and E (e) are the complete elliptic integrals of the first and second kind. For railway application, these integrals can be used in tabulated form. The parameter represents the eccentricity of the contact ellipse $e = \sqrt{1-\left(b/a\right)^2}$ and G is the combined modulus of rigidity of the wheel and the rail [35]:

$$\frac{1}{G} = \left(\frac{1-{v_w}^2}{E_w} + \frac{1-{v_r}^2}{E_r}\right) \ldots\ldots\ldots\ldots\ldots\ldots\ldots (Equation\ 3.5)$$

Where E_w and E_r are the Young's modulus, and v_w and v_r are the Poisson's ratios of the wheel and the rail, and which are equal in the case of steel wheel and steel rail [35].

The values of the semi-elliptical radii are given by:

$$a = m\left(\frac{3\pi F_n}{4G(A+B)}\right)^{\frac{1}{3}},\ b = n\left(\frac{3\pi F_n}{4G(A+B)}\right)^{\frac{1}{3}}$$

The coefficients m and n in are given by Hertz (see Kalker [1990]). The total deformation of two contacting bodies is given as:

$$\delta = \frac{p_0 b}{G}K(e) \ldots\ldots\ldots\ldots\ldots\ldots (Equation\ 3.6)$$

Once the ratio of the elliptical radii is calculated, the normal force is given by:

$$F_z = K_H\delta^{\frac{3}{2}} = \delta^{\frac{3}{2}}\left(\frac{9}{16R_eG^2}\right)^{\frac{-1}{2}} F^{\frac{-3}{2}}{}_2 \ldots\ldots\ldots\ldots\ldots\ldots (Equation\ 3.7)$$

Where K_H is Hertzian spring stiffness and in which factors F_2 and F_1 are given by :

$$F_2 = \frac{2}{\pi}\sqrt{\frac{b}{a}}\ {F_1}^{-1}\ K(e),$$

$$F_1 = \frac{4}{\pi e^2}\left(\frac{b}{a}\right)^{\frac{3}{2}}\left[\left(\left(\frac{b}{a}\right)^2 \boldsymbol{E}(e) - \boldsymbol{K}(e)\right)(\boldsymbol{K}(e) - \boldsymbol{E}(e))\right]^{\frac{1}{2}}$$

- $A + B = \frac{1}{2}\left(\frac{1}{R_W} + \frac{1}{\infty} + \frac{1}{R_r} + \frac{1}{\infty}\right)$ = 0.00286/mm

  $$A - B = \frac{1}{2}\sqrt{\left(\frac{1}{R_W} - \frac{1}{\infty}\right)^2 + \left(\frac{1}{R_r} - \frac{1}{\infty}\right)^2 + 2\left(\frac{1}{R_w} - \frac{1}{\infty} * \frac{1}{R_r} - \frac{1}{\infty}\right)COS2\psi}$$ = 0.000476/mm

  The angle of ψ is between the radius of the wheel and rail which is taken as $\frac{\pi}{2}$ for this case:

  $$cos\theta = \frac{B-A}{A+B} = 0.166$$

  $$\theta = COS^{-1}\ 0.166$$

$\theta = 80.8^0$

By using the following table (the Hertz coefficient) and linear interpolation method the Value of m and n for the chosen rail can be easily obtained.

θ_1=80°, m_1=1.128, n_1=0.893, θ_2=85°, m_2=1.061, n_2=0.944 (Hertz coefficient Table)

$m = m_1 + \frac{m_2 - m_1}{\theta_2 - \theta_1}(\theta - \theta_1)$

m = 1.123

$n = n_1 + \frac{n_2 - mn_1}{\theta_2 - \theta_1}(\theta - \theta_1)$

n= 0.897

Inserting the obtained values the elliptical radii values can be obtained:

$$a = m^3 \sqrt{\frac{3\pi W(K_w + K_r)}{4(A+B)}}$$

$$b = n^3 \sqrt{\frac{3\pi W(K_w + K_r)}{4(A+B)}}$$

Where Kr and Kw are the constant modules of rail and wheel respectively that depends on material property and W is the normal applied load on the wheel rail contact:

$K_W = \frac{1-{v_w}^2}{\pi E_w}$, $K_r = \frac{1-{v_r}^2}{\pi E_r}$

W = 11.5 ton* 1000* 9.8 /2 = 53900 N

Inserting the calculated values in to the above equations:

$a =$ 5.88mm

$b = 4.01mm$

3.2. Kinematic Analysis

In a kinematic analysis of the wheel the angular velocity, the time required for braking and the braking distance of the wheel will be calculated;

$$v(t) = v_0 - at$$

$$v(t) = 22.2 - 4.44t\ m/sec$$

Angular velocity of the wheel

$$\omega = \frac{v_0}{r_w} = \frac{22.2}{0.3} = 74\ rad/sec$$

Time needed for braking

$$t_b = \frac{v_0}{a}\ where\ v_f = 0$$

$$t_b = \frac{22.2}{4.44} = 5sec$$

Braking distance

$$s = \frac{v_f^2 - v_0^2}{2a}\ [\ v_f = 0\ ]$$

$$s = -\frac{v_0^2}{2a} = \frac{22.2^2}{2 * 4.44} = 55.5\ m$$

Calculating for the angular velocity of the wheel at time t

$$\omega(t) = \frac{v(t)}{r_w}$$

$$\omega(t) = \omega_0 \left(1 - \frac{t}{t_b}\right)$$

$$\omega(t) = 74\ (\ 1 - \frac{t}{5sec}\ )$$

$$\omega(t) = 74 - 14.8t\ rad/sec$$

Frictional force between the wheel and rail

$F_f = F_b * \mu_b$

$F_f = 56300 * 0.3$

$F_f = 16890\ N$

Torque on the wheel

$T_b = F_f * r_w$

$T_b = 16890 * 0.3$

$T_b = 5067\ Nm$

3.3. Thermal loading

The initiation and propagation of surface cracks is highly influenced by the presence of thermal loads. In railway wheels, the thermal load is normally increased during braking operation. When brakes are applied, the temperature rises, causing the fatigue strength of the material to drop. Thermal loading may induce cyclic and residual tensile stresses near the running surface of the wheel which will promote both the initiation and the early growth of a surface crack. It should be noted that resulting residual stresses due to thermal loading are also influenced by the geometrical design of the wheel. When thermal loading is the dominant cause to fatigue, resulting surface cracks tend to be radial. However, the point of initiation of such cracks is not restricted to the tread, but varies and even includes the bottom of the flange side. For rails, thermal damages are more rare, but can occur as "wheel burns" when wheels are sliding at stop signals [44, 45, 46, 47].

Martensite formation on the wheel tread normally indicates a previous history of temperatures which were high enough to austenite the material (above some 700◦C) and fast cooling of the wheel. However, martensite can also form due to rapid shear under impacting. Extensive martensite is typically caused by locking and sliding of the wheel due to frozen breaks, leaves on the track [47].

From several studies of thermal loading reports, thermal loading can be controlled by several mechanisms such as; experimental evaluation of high temperature fatigue resistance of wheel

steel, measurement of thread face temperature in operation, analysis of stress and strain due to thermal and mechanical loading and development numerical fatigue prediction models based on continuum mechanics and fracture mechanics [47].

Frictional heating and temperature calculation

The temperature rise due to frictional heat generation at the interface of two sliding components plays an important role in determining their performance and life. Accurate knowledge of the temperature rise is critical for performing thermal stress analysis between two sliding bodies [44].

While the maximum surface temperature would generally be of greater interest, a prediction of the average interface temperature over the contact region can also be useful, as it is well correlated with the peak temperatures and may be easier to experimentally verify. In any case, a prediction of the maximum and/or average steady state temperature rise at the interface of two sliding bodies can be valuable in designing against fatigue failure or other modes of system breakdown [44-46].

The maximum surface temperature during rolling contact of railway wheels with sliding friction can be estimated using ***Blok's flash temperature*** formula. For a more detailed investigation, semi-analytical and numerical methods are available. A survey of various methods is given and an efficient approach is proposed for Hertzian contact [46].

Flash temperature is the sharp temperature rise that takes place at the interface between two rubbing solids upon motion. Solid surface irrespective of their method of formation contains irregularities of deviation from a prescribed geometrical form. The high points on the surfaces are referred to as asperities and the low points are referred to as valleys. Upon sliding of the mating surfaces relative to each other, heat will be generated. Generation of heat causes those asperities in contact to act as heat sources. Heat generation at a given contact point is a very rapid process, therefore, heat source act almost instantaneously. Due to the local reduction in contact area, a construction in path of conducted heat takes place. Constricting the path of conduction increases the density of thermal flux lines at the true contact spots. This effect causes thermal spikes (temperature flashes) upon sliding, where asperities interlock. The temperature spikes or flashes are of short duration and are typically of high magnitude. The term was coined by Harmen Blok in 1937 [46].

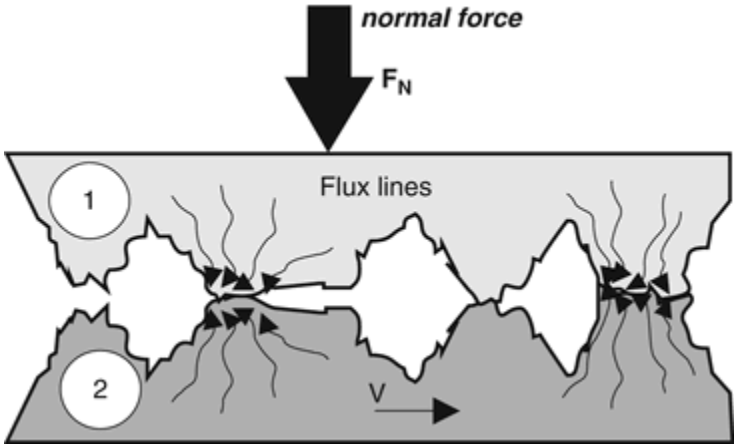

Figure 3.1. Flux lines at the asperity contacts of two rubbing solids [46]

Even though, Blocks "Flash temperature theory" is our basis for calculation of temperature on two contacting bodies, all works on wheel/rail contact are confined to smooth surfaces and most of these are based on the theory of Hertz for contact mechanics problems. But real surfaces are always rough. Using measured profiles of rough surfaces, even the calculation of stress and strain demands computer simulations. With smooth surfaces, the heat conduction can be treated one-dimensionally, but for rough surfaces, this simplification is not possible, and the investigation of temperatures is also a very complicated numerical problem. On the other hand, Archard has already stated that the influence of surface roughness can be neglected to a first approximation, since the largest temperatures are those deduced for the whole region rather than those deduced for the smaller individual contact areas [46].

Analytical solution for constant heat flow rate between wheel and rail

Table 3.1. Reference data for Calculation of maximum Temperature

	Symbol	Value	Unit
Thermal diffusivity [46]	κ	$14.2 * 10^6$	m^2/s
Sliding velocity (longitudinal) [46]	v_s	22.2	m/s
Density of wheel	ρ	7300	$kg\ /m^3$
Coefficient of friction	μ	0.3	1
Thermal conductivity	λ	50	W/Km
Normal force	F_Y	56.3	KN

Maximum Hertizian pressure	p_0	925.6	Mpa
Semi – axis of contact ellipse (rolling direction)[46]	a	5.88	mm
Semi –axis of contact ellipse (lateral direction)[46]	b	4.01	mm
Initial wheel temperature	T^o	40	^{0}c
Ambient temperature	T^o	20	^{0}c
Deceleration	a	4.44	m/sec^2

Total heat generation on the wheel

$Q_{gen} = Energy\ on\ the\ wheel$

$Q_{gen} = T_w * \omega\ (t)$

$T_b = F_f * r_b$

$F_f = F_b * \mu_b$

$Q_{gen} = F_b * \mu_b * r_b * \omega\ (t)$

$Q_{gen} = F_b * \mu_b * r_b * (74 - 14.8t)$

$Q_{gen} = 56300 * 0.3 * 0.3 * (74 - 14.8t)$

$Q_{gen} = 374958 - 74991.6\ t\ joul$

Heat flux on the wheel

$$q_t = k_d * \frac{Q_{gen}}{Area} = 0.51 * \frac{374958 - 74991.6\ t}{\pi * 0.00588^2}$$

$q_t = 5531633786.52 - 1106326873.01t\ {joul}/{m^2}$

3.4. Plastic Deformation

When the stress applied on a material exceeds its elastic limit, it imparts permanent non-recoverable deformation called ***plastic deformation*** in the material. Microscopically it can be said of plastic deformation involves breaking of original atomic bonds, movement of atoms and the restoration of bonds. I.e. plastic deformation is based on irreversible displacement of atoms through substantial distance from equilibrium position.

On a straight track, the wheel is in contact with the top of the rail, but in curves, the wheel flange may be in contact with the gauge corner of the rail. The wheel load is transmitted to the rail through a tiny contact area under high contact stresses. This results in repeated loading above the elastic limit, which leads to plastic deformation. The depth of plastic flow depends on the hardness of the rail and the severity of the curves; it can be as much as 15 mm [34].

When a material is subjected to repeat loading, its response depends on the ratio of the amplitude of the maximum stress to the yield stress of the material. When the load increases above the elastic limit, the contact stresses exceed yield and the material flow plastically. After the wheel has passed, residual stresses will develop. These residual stresses are protective in nature in that they reduce the tendency of plastic flow in the subsequent passes of the wheel [34].

For crystalline materials deformation is accomplished by means of a process called slip that involves motion of dislocations. In amorphous materials plastic deformation takes place by viscous flow mechanics in which atoms slide pass one another under applied stress without any directionality.

Plastic deformation, as elastic deformation can be characterized by defining the relation between stress and the corresponding strain. A *constitutive equation* can be used to determine the relation for plastic zone.

For a plastic zone, stress is not only a function of strain as in elastic zone; rather it also depends on temperature, microstructure, strain rate and other material properties [34].

$$\sigma = f(\chi, T, microstructure, \dot{\chi})$$

Where x: strain, T: temperature and $\dot{\chi}$: strain energy

$$\sigma = kx^n \quad \text{..... (Equation 3.14)}$$

K – Strength coefficient

n – Strain hardening exponent

n = 0; perfectly plastic

n= 1; perfectly elastic

For most metals n is between 0.10 and 0.50 [34].

The power law equation described above known as Holloman- Ludwing equation

- Another power law equation which describes the material behavior when strain-rate effect is prominent.

$$\sigma = k\dot{x}^m \dots\dots\dots\dots\dots\dots (Equation\ 3.15)$$

Where; m = index of strain rate sensitivity

m = 0.2 for common metal

m= 0.4-0.9 for super plastic behavior

$$\sigma = k\ (x_0 + x)^n \dots\dots\dots\dots (Equation\ 3.16)$$

ε_0 = strain of material had undergone before the present characterization

Finally the power law equation can be simplified to;

$$\sigma = \sigma_0 + kx^n \dots\dots\dots\dots\dots (Equation\ 3.17)$$

σ_0 = yield strength of material where plastic strain is zero.

CHAPTER 4: MODELING AND ANALYSIS

4.1. Analysis Assumptions

The analysis section consists of modeling of the wheel/rail using finite element modeling (FEM). This section enables to see the influence of chemical composition (material) on plastic deformation and spalling due to mechanical and thermal loading.

The following approximations have been made to reduce the computational Complexity:

1. No rotational motion is considered;
2. No abrasion was considered;
3. The coefficient of sliding friction was assumed not to change with load and temperature;
4. A simplified wheel model was used.

The following assumptions also made to obtain the heat partition distribution and thus the temperature rise at the interface;

I. The bodies in contact are modeled as homogeneous, isotropic, elastic half-spaces as it relates to their temperature responses to surface heat flow and deformation responses to surface stress.
II. A constant coefficient of kinetic friction exists that serves as the proportionality factor between interfacial shear stress and contact pressure.
III. The bodies have matching temperatures at every point within the contact zone.
IV. Heat losses due to convection and radiation are negligible.

4.2. Wheel and Rail Modeling

The wheel and rail are modeled from the data obtained from AALRT depot. They are modeled by finite element modeling and analyzing software called ABAQUS.

The coordinate system used in this software

X – axis (lateral axis)

Y – axis (vertical axis)

Z – axis (longitudinal axis) as convention

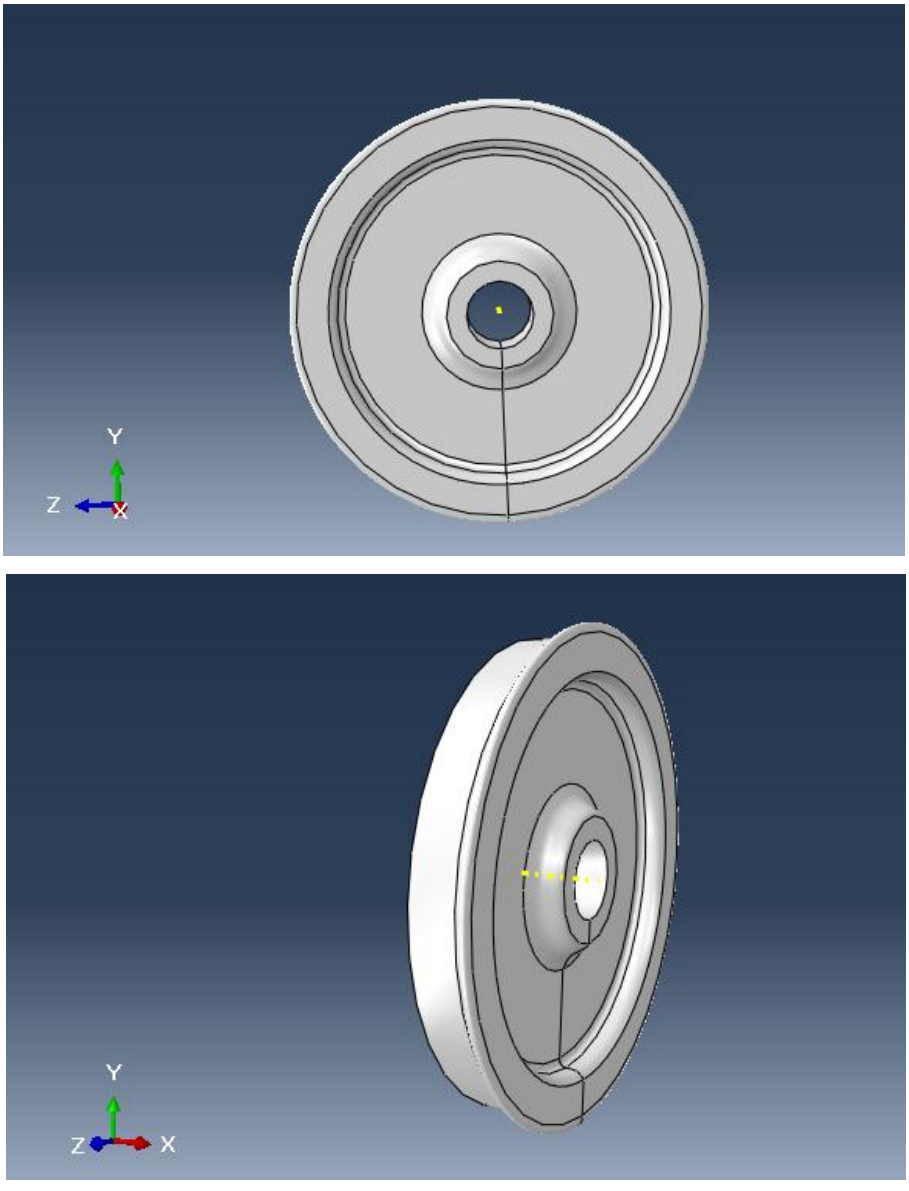

Figure 4.1 Wheel models of AALRT train using ABAQUS

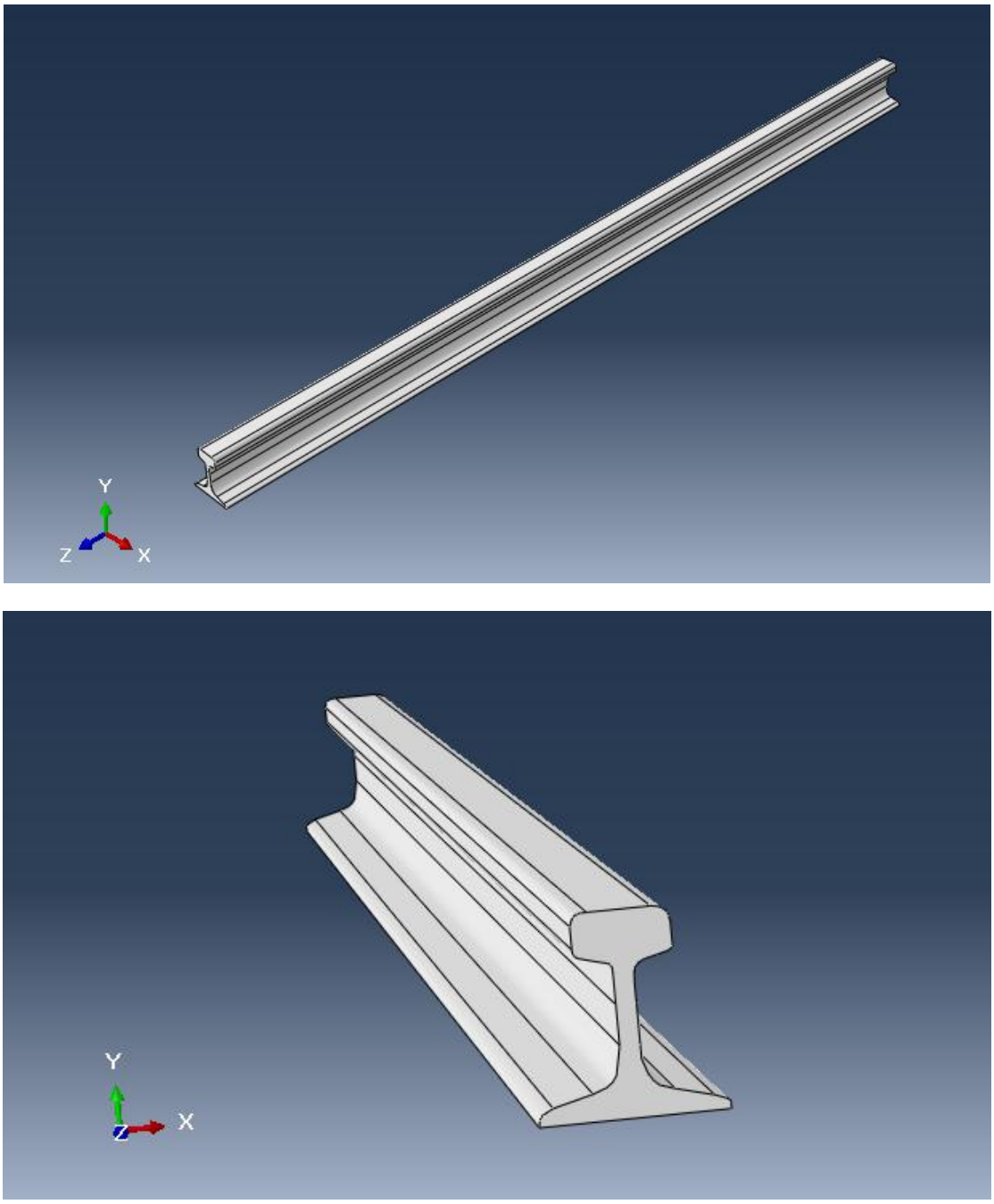

Figure 4.2. Rail model of AALRT train using ABAQUS

4.3. Finite element Modeling (FEM)

The finite element modeling section involves analyzing the wheel by software that is programed for FEM modeling and analysis. In this research ABAQUS is the software used for FEM.

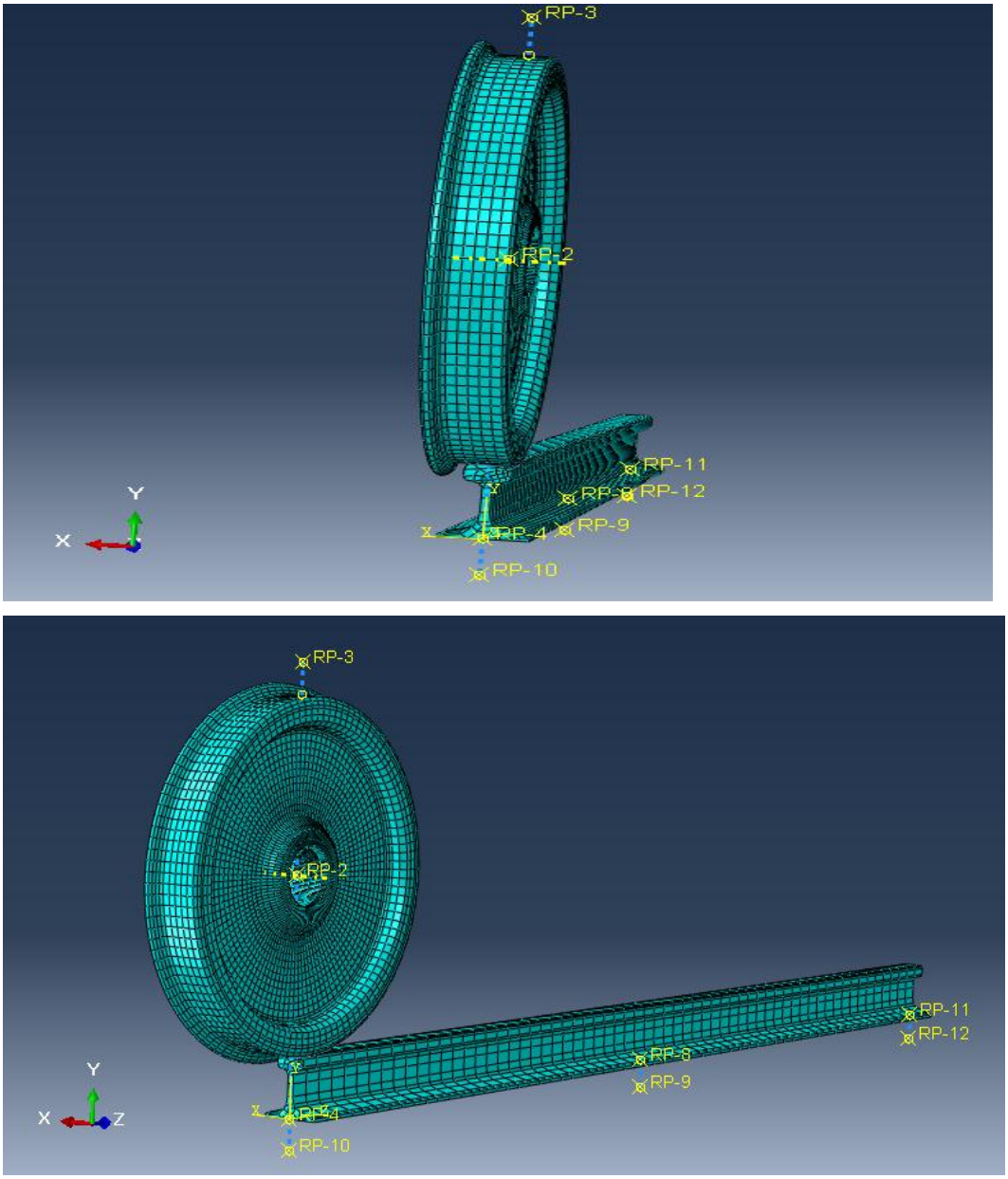

Figure 4.3. FEM model of wheel rail assembly using ABAQUS

4.4. Software simulation and Mathematical Analysis

This section of the research analyzes the influence of chemical composition by comparing three wheel carbon steels which are selected from the UIC-wheel standard. UIC- wheel standard puts a grade for wheels with different carbon weight percentage that is used for different train applications. UIC- standard puts high grade carbon wheel material for a train operates under high load, low speed and high braking application. For a train operates under light load and moderate speed with moderate braking condition, the carbon grade lowered.

The materials selected for this analysis are wheels that are used for passenger light rail application. They have a different carbon weight percentage that prominently makes a difference in hardness value. They also have a difference in weight percentage of silicon, manganese and other wheel alloying elements. From the above literatures in studies silicon primarily used for stabilizing temperature rise by delaying the time for austenitization. These and other parameters will be analyzed using ABAQUS for the three wheel materials.

Table 4.1. Wheel classes of UIC standard for different train applications [51]

Class	W % C	BHN	Service condition
L	≤ 0.47	197-277	Light weight wheel loads, high speed service, more sever braking conditions than other classes
A	0.47-0.57	255-321	Moderate wheel loads, high speed service, service braking conditions
B	0.57-0.67	277-341	Heavy wheel loads, high speed service, sever braking conditions
C	0.67-0.77	321-363	(1) High wheel loads under light braking (2) Heavier braking conditions employing off-thread brakes

The analysis using the software ABAQUS involves the following basic steps.

1. Sketching the two dimensional geometry and create a 3D part representing the models

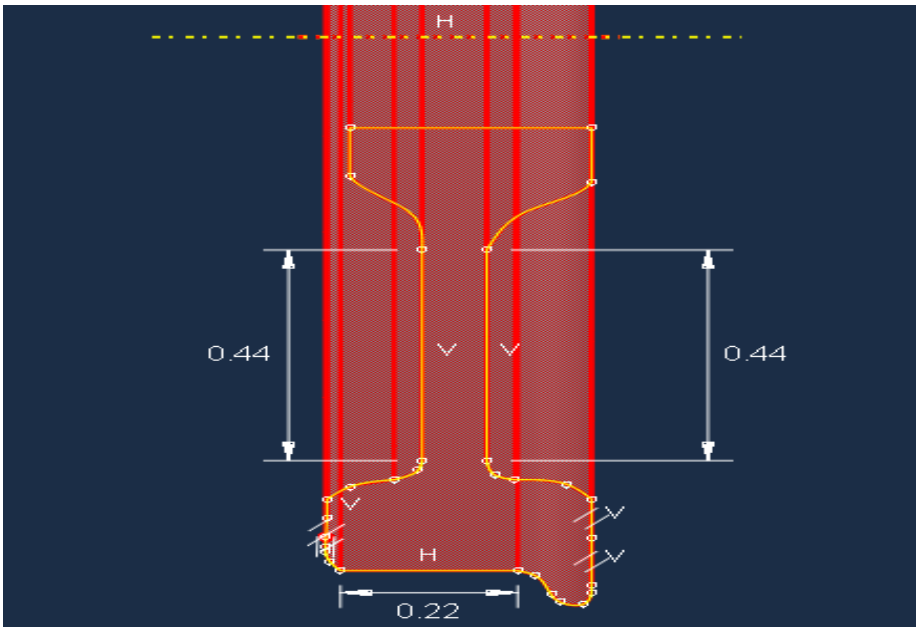

Figure 4.4. Wheel 2D modeling on ABAQUS

2. Define the material properties and section properties of the models

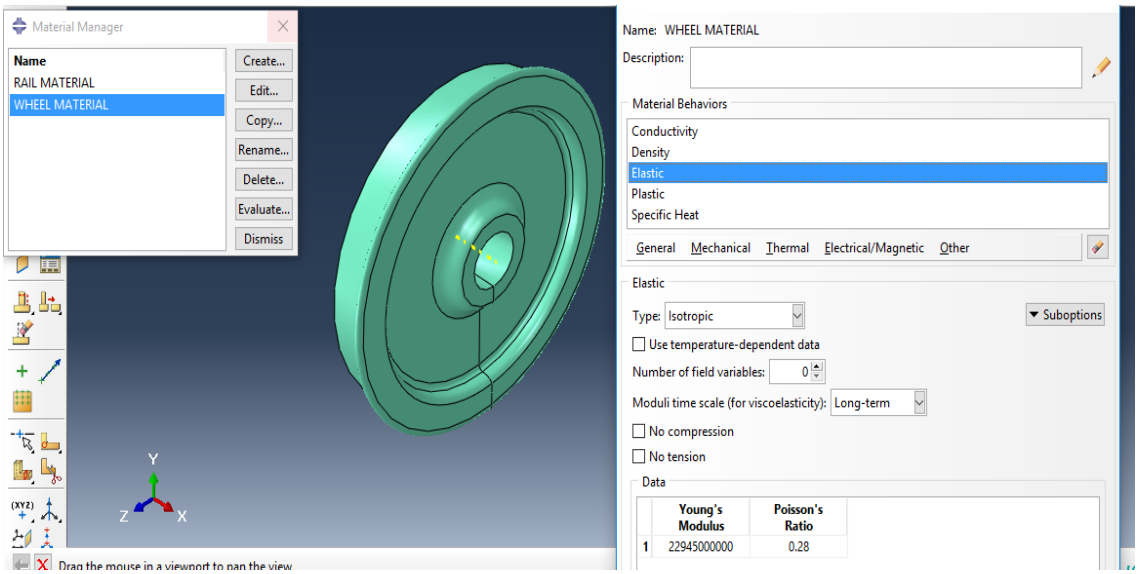

Figure 4.5. Material property and section property of wheel

3. Assemble the models

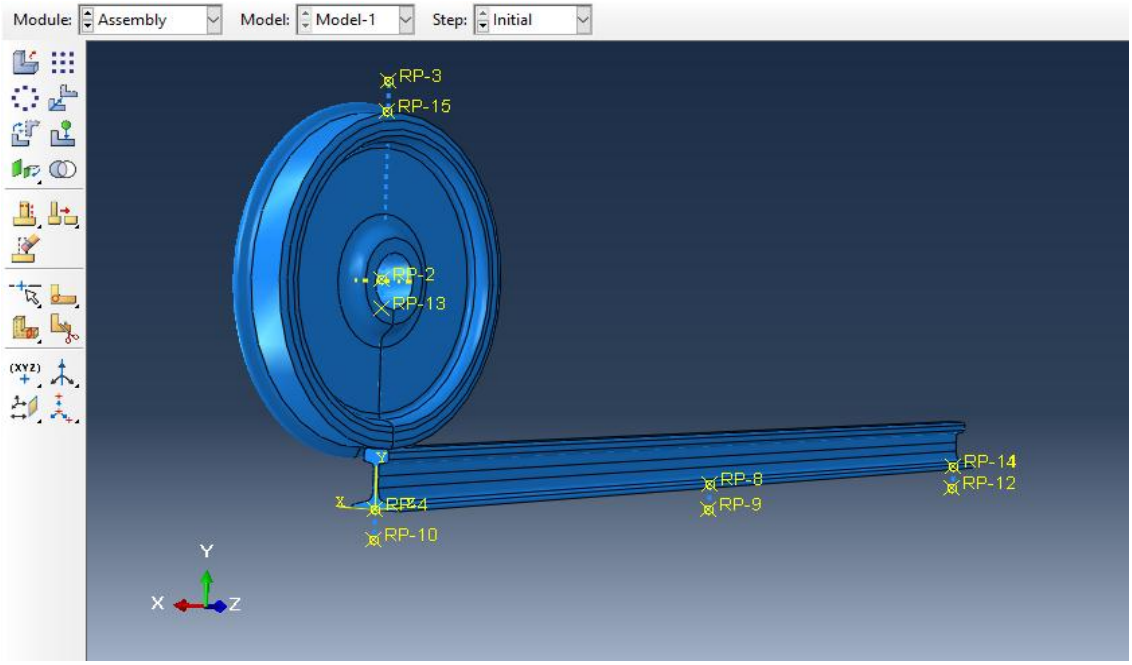

Figure 4.6. Wheel rail assembly on ABAQUS

4. Configure the analysis procedures and output request

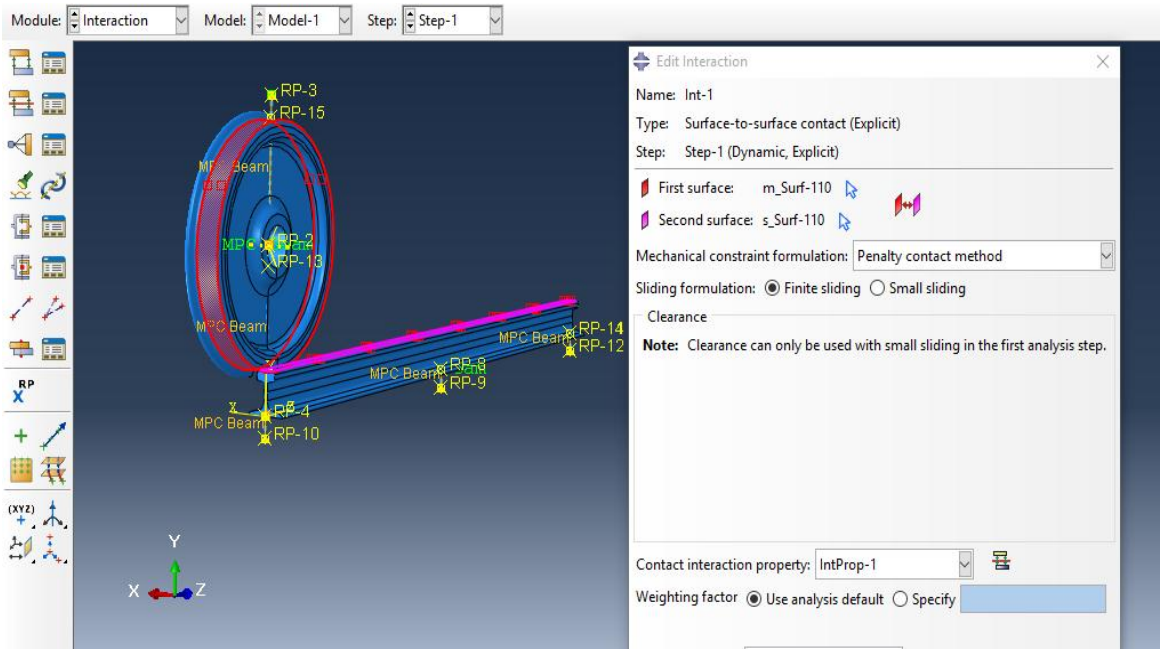

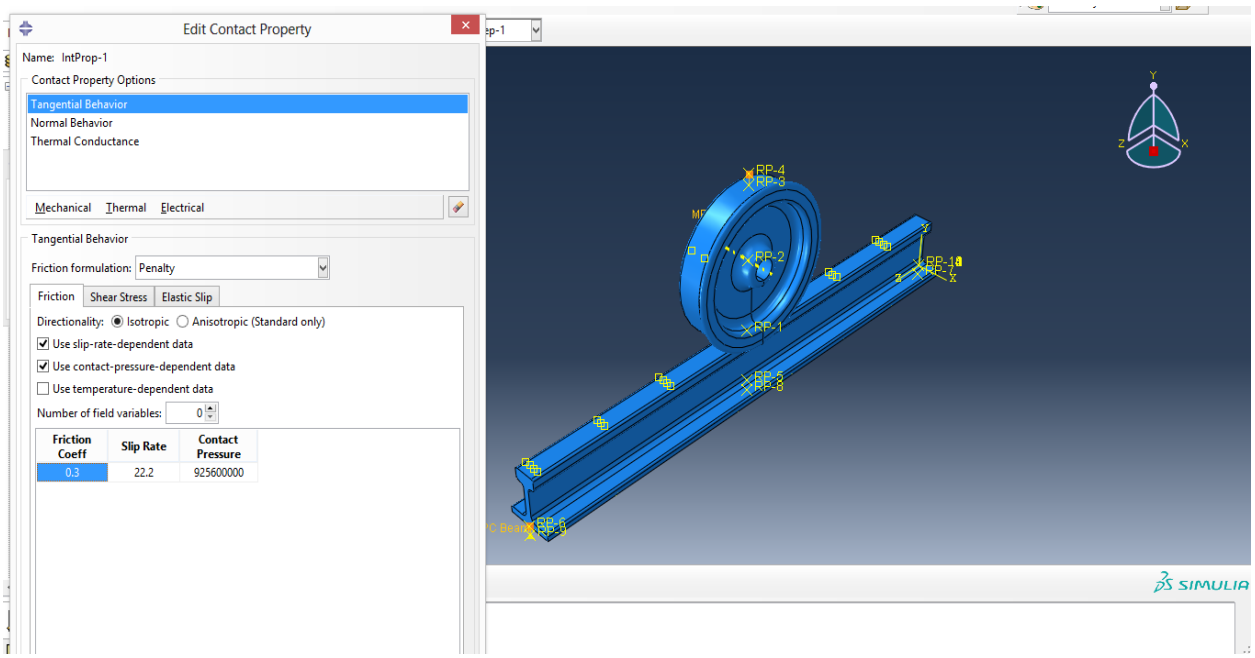

Figure 4.7. Wheel rail interaction procedure on ABAQUS

5. Apply loads and boundary conditions to the assembled model

Loads on the wheel

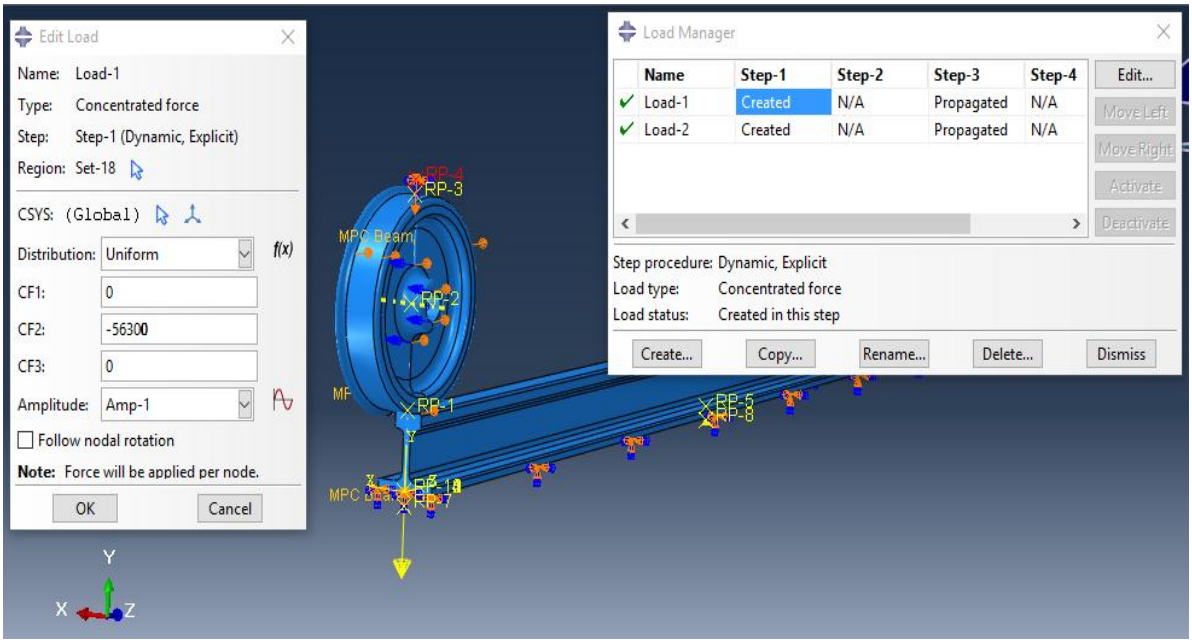

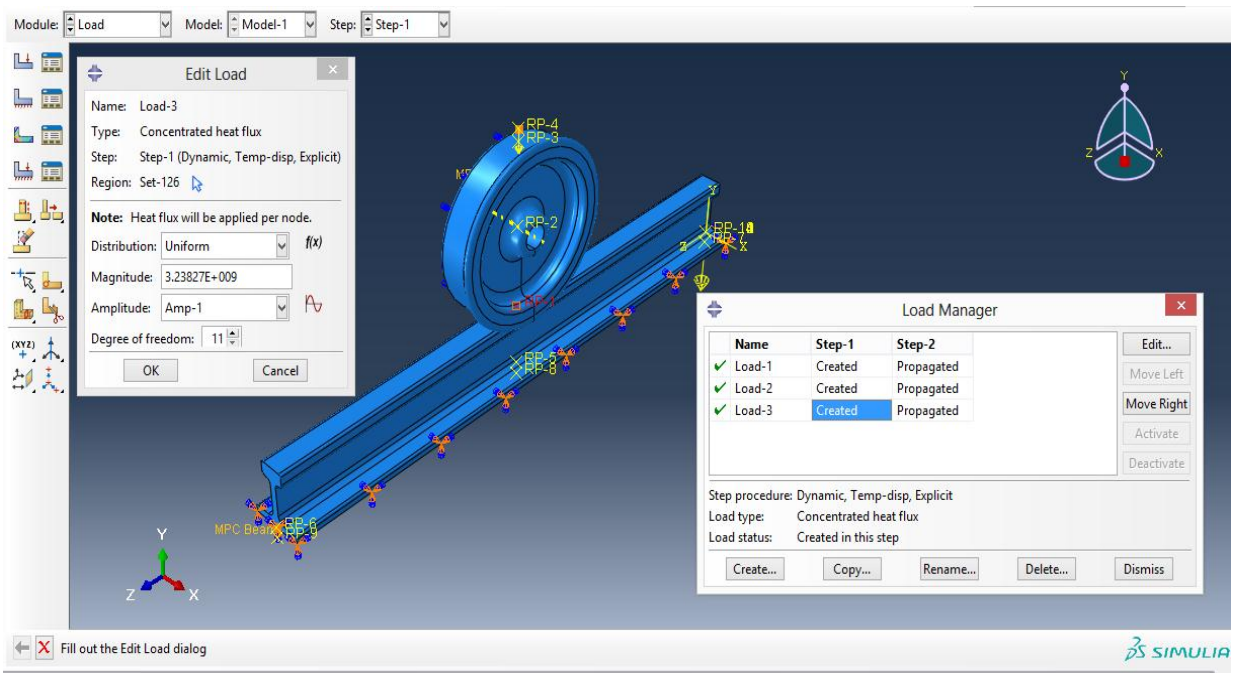

Boundary conditions for the wheel

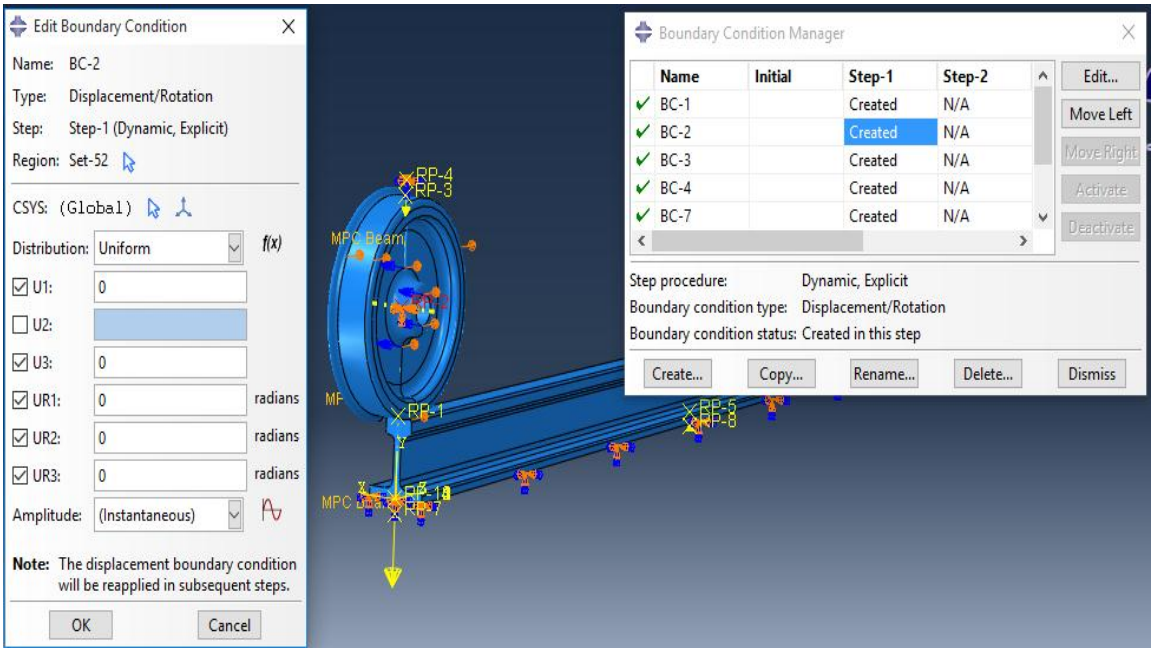

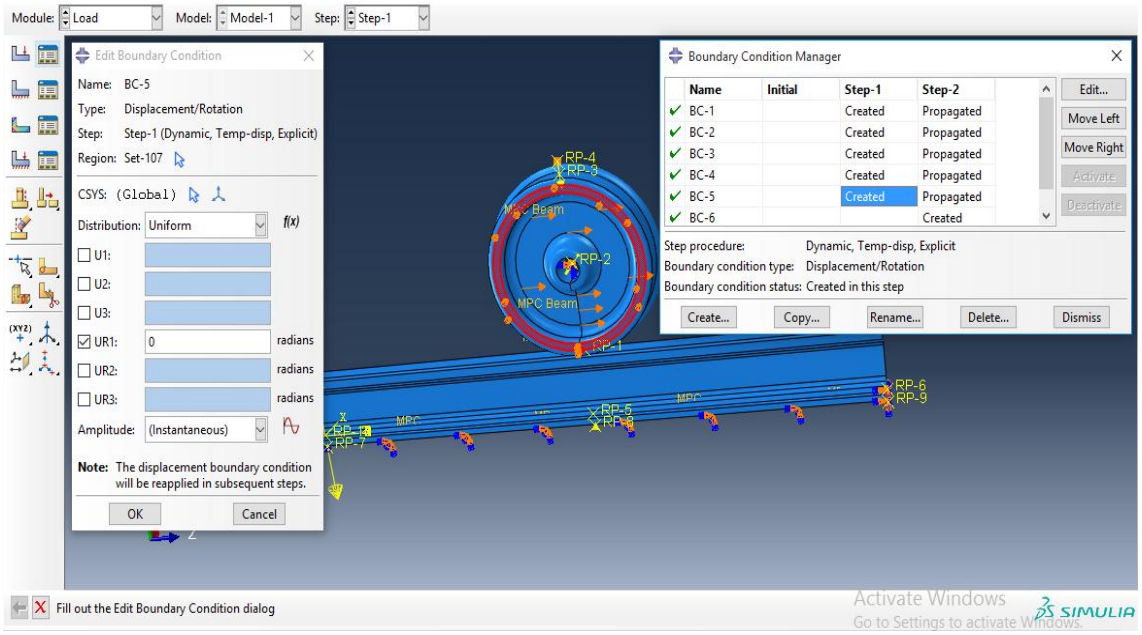
Module: Load
Model: Model-1
Step: Step-1
Edit Boundary Condition
Name: BC-5
Type: Displacement/Rotation
Step: Step-1 (Dynamic, Temp-disp, Explicit)
Region: Set-107
CSYS: (Global)
Distribution: Uniform
U1:
U2:
U3:
UR1: 0 radians
UR2: radians
UR3: radians
Amplitude: (Instantaneous)
Note: The displacement boundary condition will be reapplied in subsequent steps.
OK
Cancel
Boundary Condition Manager
Name | Initial | Step-1 | Step-2
BC-1 Created Propagated
BC-2 Created Propagated
BC-3 Created Propagated
BC-4 Created Propagated
BC-5 Created Propagated
BC-6 Created
Edit...
Move Left
Move Right
Activate
Deactivate
Step procedure: Dynamic, Temp-disp, Explicit
Boundary condition type: Displacement/Rotation
Boundary condition status: Created in this step
Create...
Copy...
Rename...
Delete...
Dismiss
RP-4
RP-3
MPC Beam
RP-2
MPC Beam
RP-1
RP-6
RP-9
RP-5
RP-8
MPC
RP-7
Fill out the Edit Boundary Condition dialog
Activate Windows
Go to Settings to activate Windows.
SIMULIA

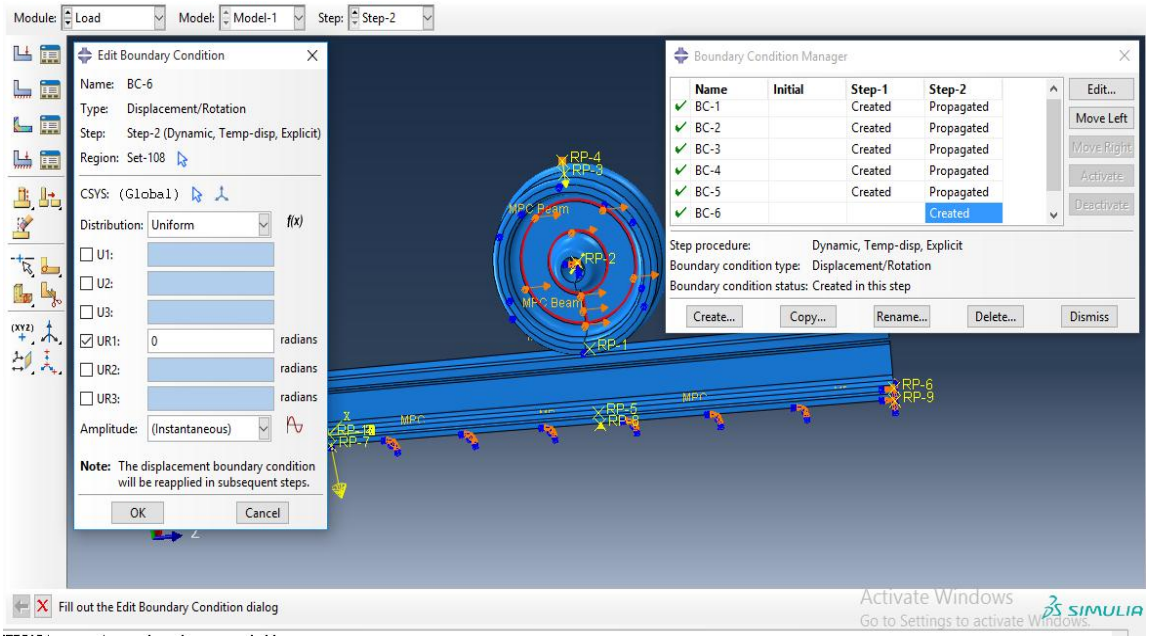
Module: Load
Model: Model-1
Step: Step-2
Edit Boundary Condition
Name: BC-6
Type: Displacement/Rotation
Step: Step-2 (Dynamic, Temp-disp, Explicit)
Region: Set-108
CSYS: (Global)
Distribution: Uniform
U1:
U2:
U3:
UR1: 0 radians
UR2: radians
UR3: radians
Amplitude: (Instantaneous)
Note: The displacement boundary condition will be reapplied in subsequent steps.
OK
Cancel
Boundary Condition Manager
Name | Initial | Step-1 | Step-2
BC-1 Created Propagated
BC-2 Created Propagated
BC-3 Created Propagated
BC-4 Created Propagated
BC-5 Created Propagated
BC-6 Created
Edit...
Move Left
Move Right
Activate
Deactivate
Step procedure: Dynamic, Temp-disp, Explicit
Boundary condition type: Displacement/Rotation
Boundary condition status: Created in this step
Create...
Copy...
Rename...
Delete...
Dismiss
RP-4
RP-3
MPC Beam
RP-2
MPC Beam
RP-1
RP-6
RP-9
RP-5
RP-8
MPC
RP-7
Fill out the Edit Boundary Condition dialog
Activate Windows
Go to Settings to activate Windows.
SIMULIA

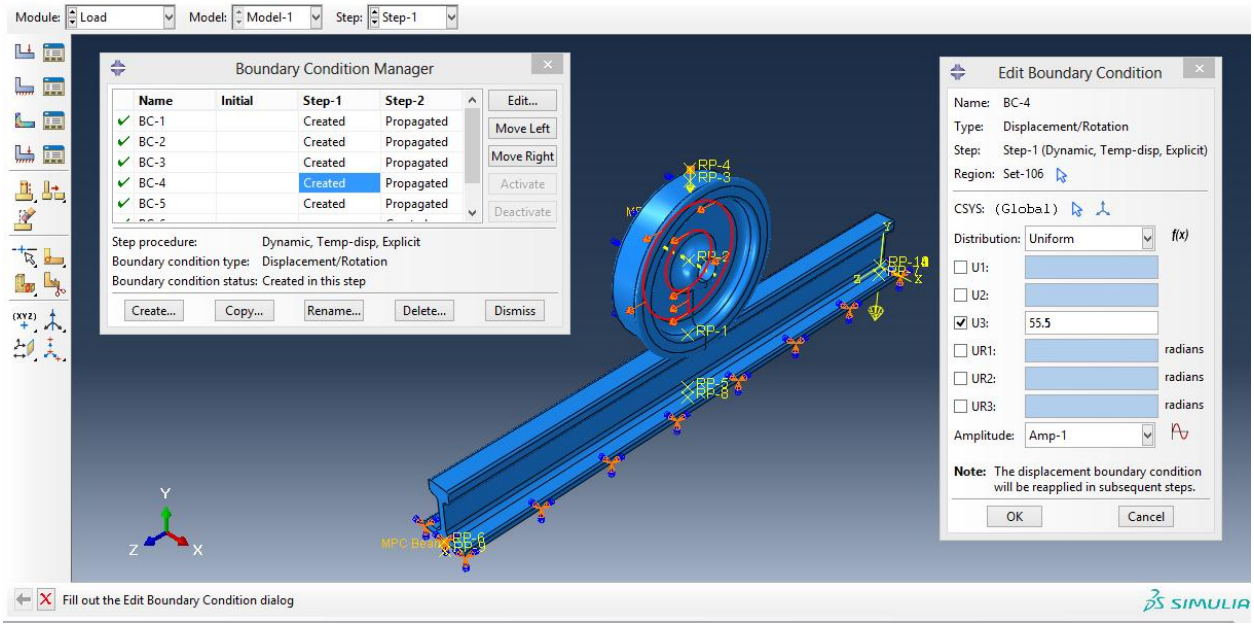

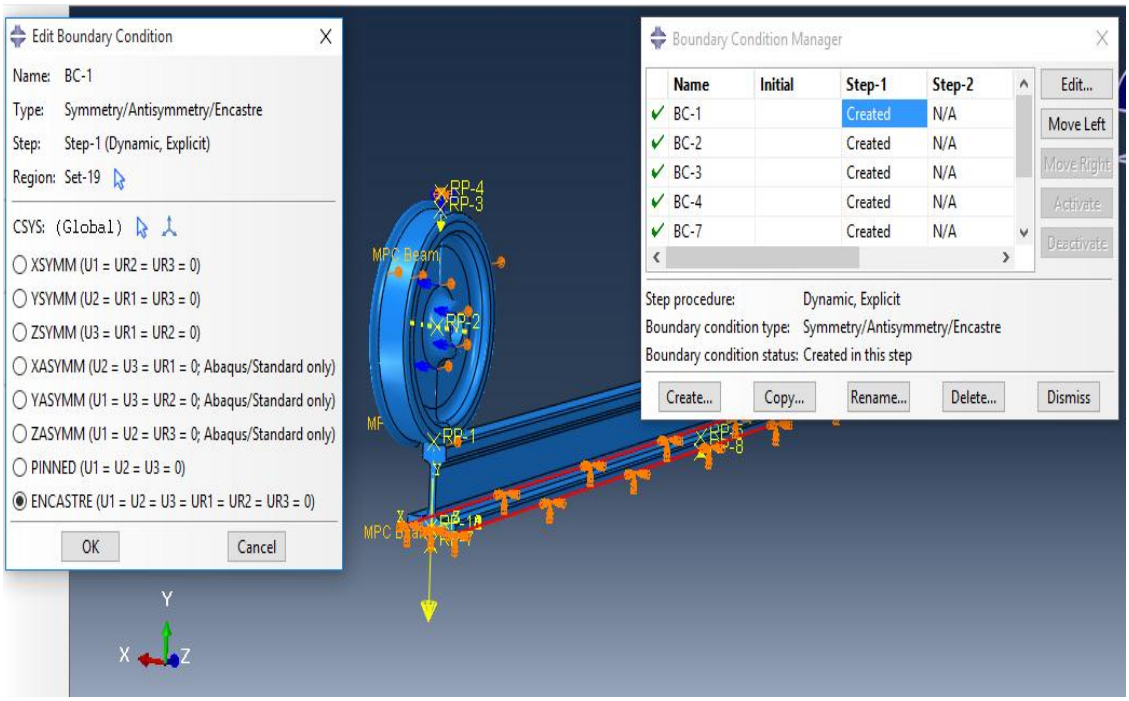

Figure 4.8. Appling load and boundary conditions on ABAQUS

6. Mesh the model

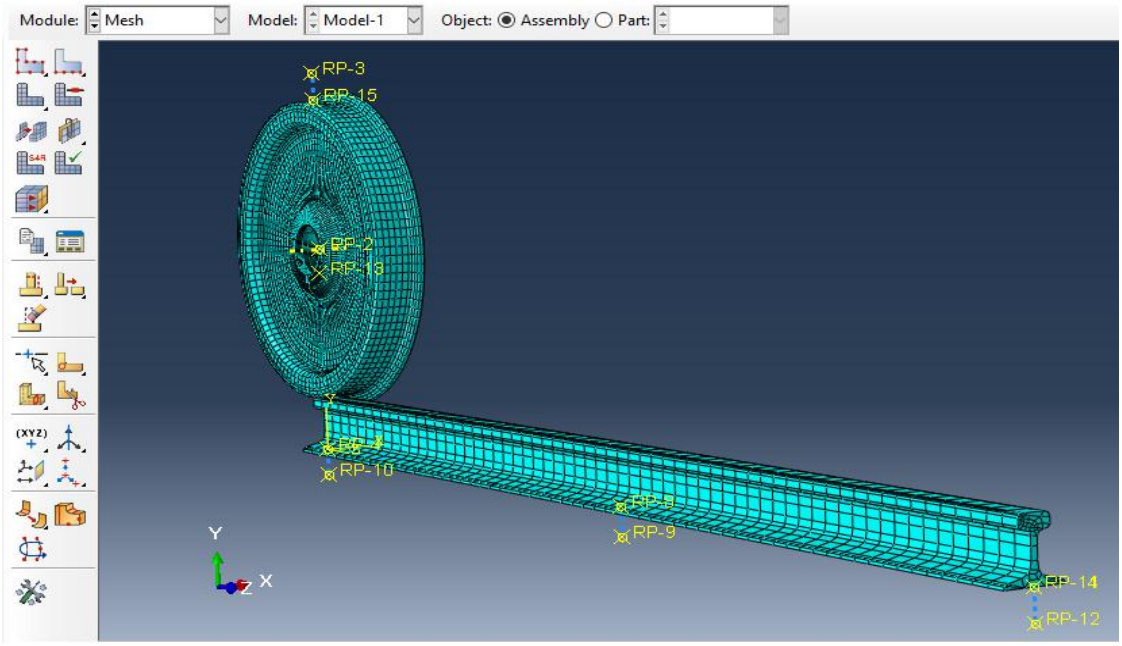

Figure 4.9. Mesh of the model

7. Create a job and submit it for analysis

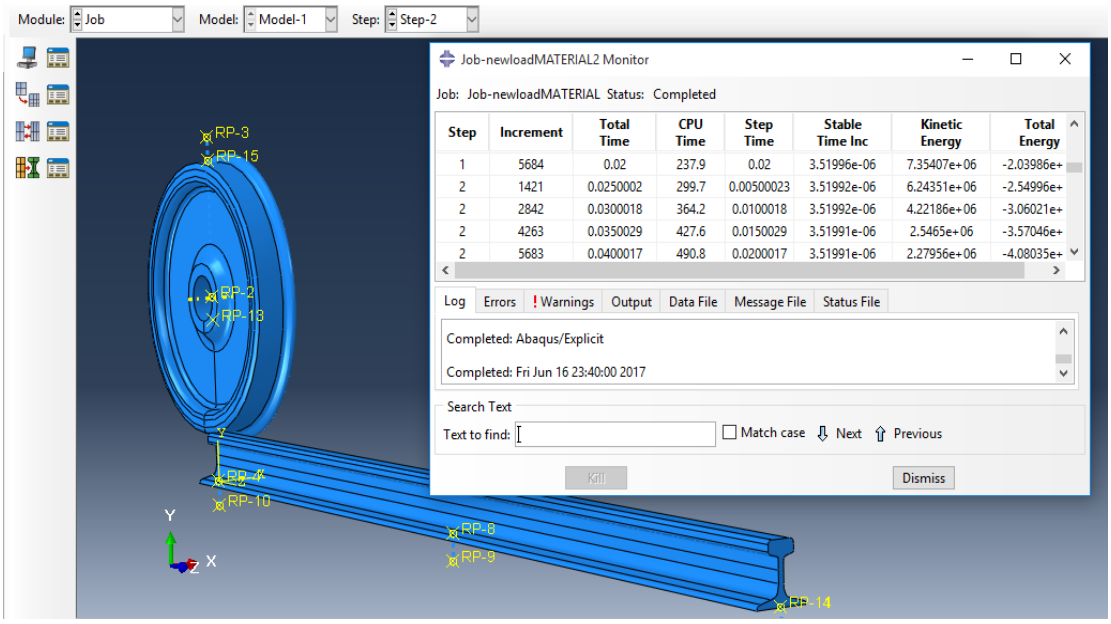

Figure 4.10. Job process on ABAQUS

8. View the results of the analysis

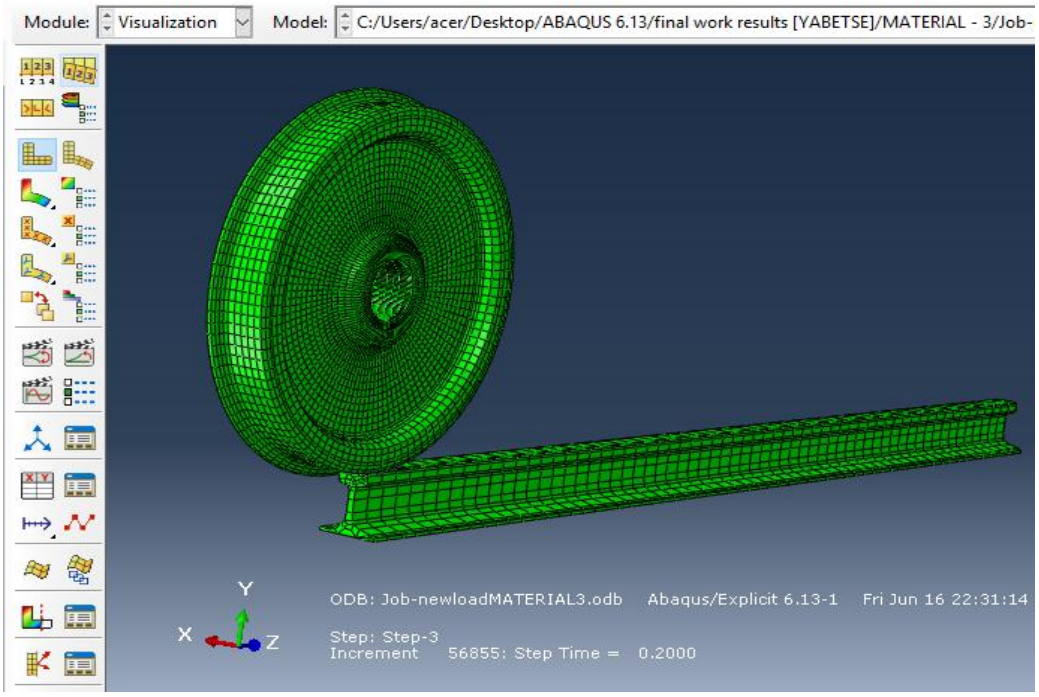

Figure 4.11. *ABAQUS analysis result*

Mechanical properties of the two sample wheels

Table 4.2. Mechanical properties of UIC standard wheels

Material (UIC 812- 3 standard)	Elastic modules [E]	Youngs modules (Gpa)	Yield strength (MPa)	Strain (elongation) %	Density (kg/m^3)	Poissons ratio (v)
MATERIAL-1 (R6T,E)	206	224.3	545	15	7800	0.285
MATERIAL-2 (R8T,E)	210	229.45	600	15	7850	0.28

Chemical composition and hardness of the two wheel samples

Table 4.4.3. Chemical compositions of UIC standard wheels

Material (UIC 812- 3) Standard	Chemical composition (Wt %)						HARDNESS (BHN)
	C	Si	Mn	P	S	V	
MATERIAL-1 R6T, E	0.50	0.1	0.8	≤ 0.05	≤ 0.05	-	200
MATERIAL-2 R8T,E	0.56	0.40	1.3	≤ 0.025	≤ 0.025	-	240

Mechanical property of UIC – 50 rails

Table 4.4. Mechanical property of UIC – 50 rails

Material	Elastic Modules (E)	Youngs modules (GPa)	Yield strength (MPa)	Strain elongation (%)	Density (kg/m^3)	Poisson's ratio (v)
UIC – 50 standard rail	210	228.55	552	18	7210	0.29

Chemical composition of UIC – 50 rails

Table 4.5. Chemical composition of UIC-50 rails

Material	Chemical composition (wt %)					HARDNESS
	C	Si	Mn	S	P	240
UIC – 50 standard rail	0.6	0.5	1.3	≤ 0.05	≤ 0.05	

Technical parameters of AALRT (Addis Ababa light rail transit) train

Table 4.6. Technical parameters of AALRT train [50]

Parameters	**Value**
Wheel diameter	660 mm
Max. Axle load	11tons
Maximum operating speed	70 km/hr.
Braking acceleration	1.14m/sec^2
Wheel thickness	120mm
Wheel thread thickness	50mm
Coefficient of friction	0.3

Calculation of input data

a. Calculation of plastic strain

In material behavior of metals the plastic zone stress-strain curve doesn't have the same slop (Elastic modulus) value with the elastic zone. The curve obeys hooks law in the elastic zone since it does have a linier curve in the stress- strain graph. On the other hand the value of plastic modules for the curve in the plastic region is calculated by a power equation. The first plastic strain values of the material will be feed to the software for further extrapolation by the software.

$$\sigma = \sigma_0 + kx^n$$

Assume $n = 0.25$

Material 1

Finding the slop of the graph using the power equation;

Take x = 0.02 for first iteration

$$545100000 = 545000000 + k0.02^{0.25}$$

$$k = 265{,}975.4468$$

Using the slope k, the other strain values will be obtained for the material

Table 4.1. Strength beyond yield limit and the corresponding plastic strain value

$\sigma(Mpa)$	$x\ (mm)$
545	0
545.1	0.02
545.14	0.076
545.18	0.20976
545.20	0.319
545.21	0.3886
545.23	0.5597
545.25	0.78053

Boundary conditions

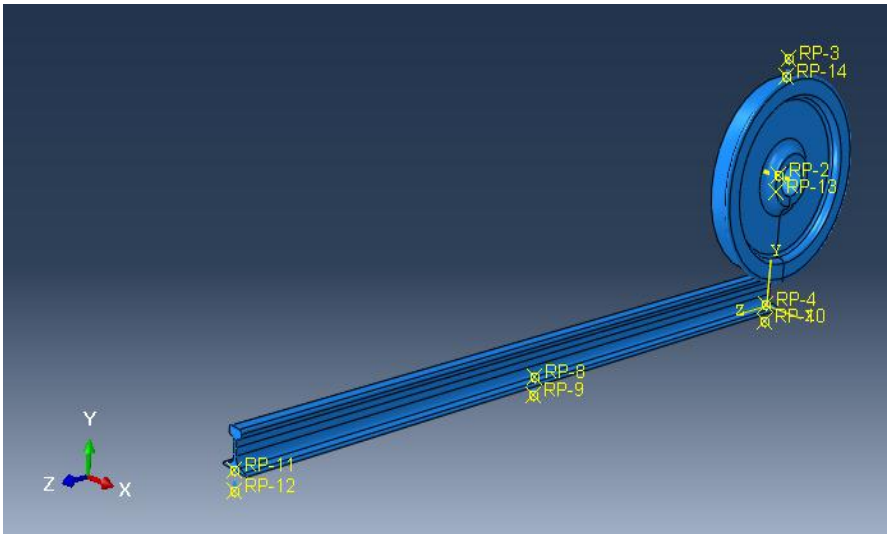

Displacement at Ux=0

Displacement at Uy=0

Displacement at Uz= 55.5m

Rotational velocity at x ;URx= 0 rad/sec at step 1

Rotational velocity at x ; URx= 0 rad/sec at step 2

Rotational velocity at y; URy=0

Rotational velocity at z; URz=0

CHAPTER 5: RESULT AND DISCUSSION

5.1. Results

1. Von misses stress (S)

MATERIAL 1

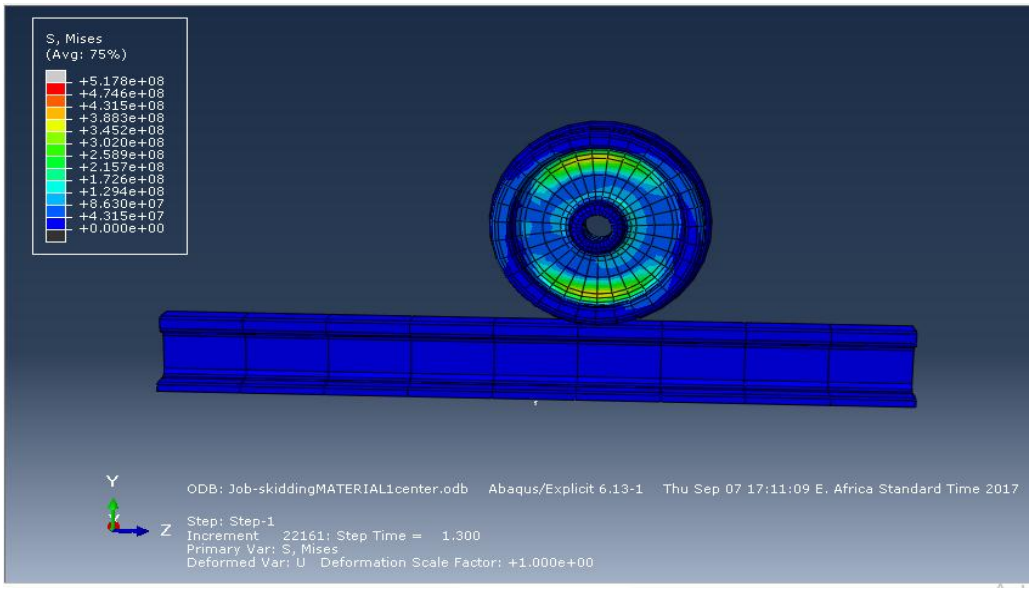

. *Figure. 5.1. Max. Von-mises stress of material 1*

MATERIAL 2

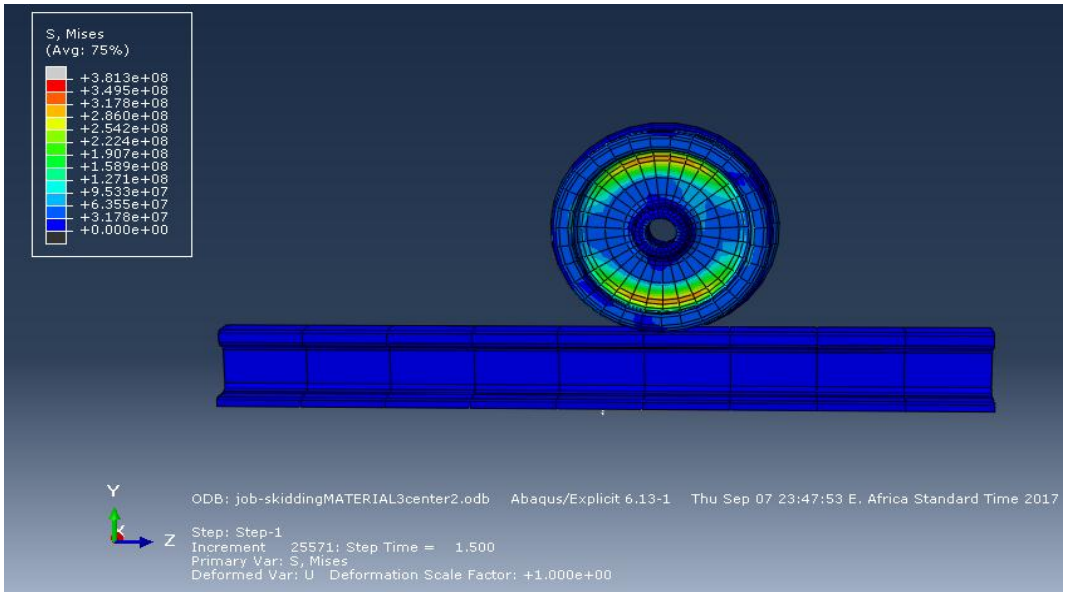

Figure 5.3. Max. Von-mises stress of material 2

2. Contact shear at surface nodes (CSHEAR 1)

MATERIAL 1

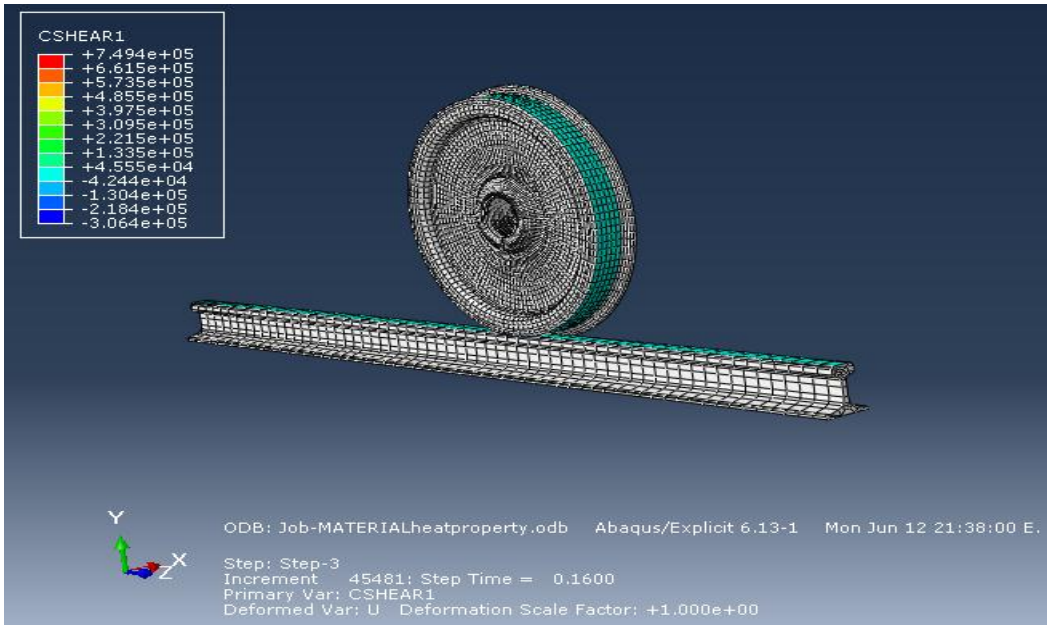

Figure 5.4. Contact shear of material 1

MATERIAL 2

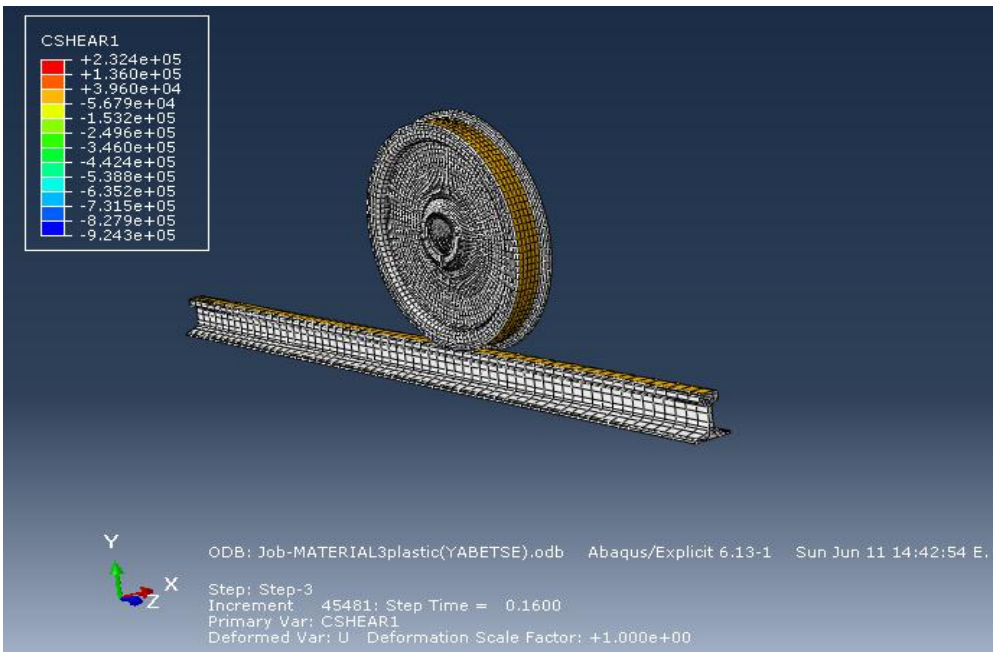

Figure 5.6. Contact shear of material 2

3. Strain at nodal components

Plastic strain on the surface (LE)

MATERIAL 1

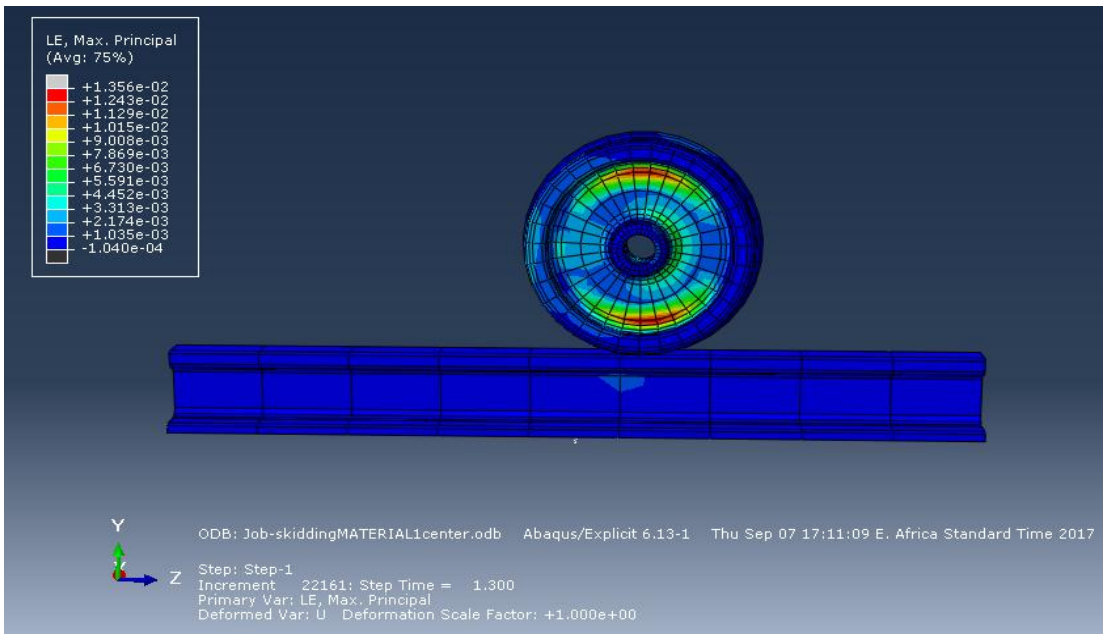

Figure 5.7. Equivalent plastic strain of material 1

MATERIAL 2

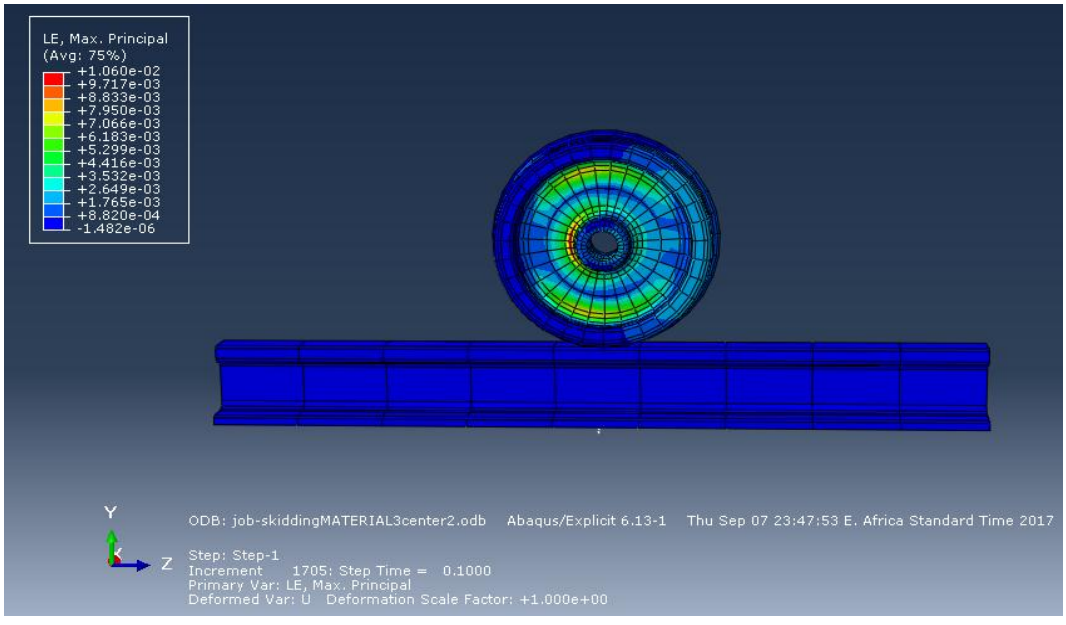

Figure 5.9. Equivalent plastic strain of material 2

4. Surface temperature at the end of the step (TEMP)

MATERIAL 1

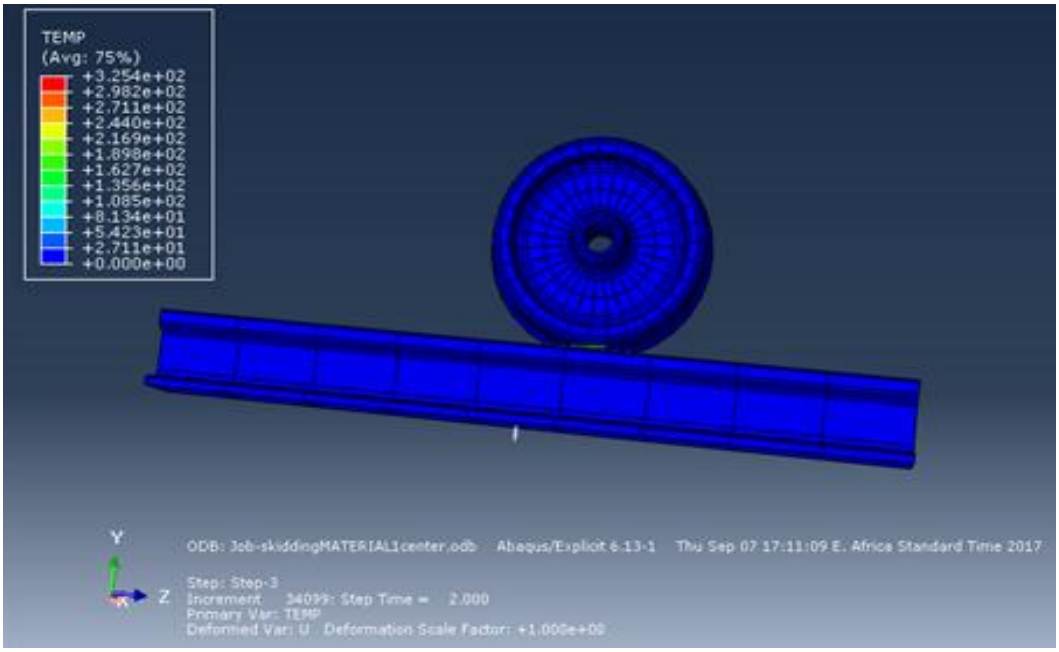

Figure 5.10. Temperature rise of material 1

MATERIAL 2

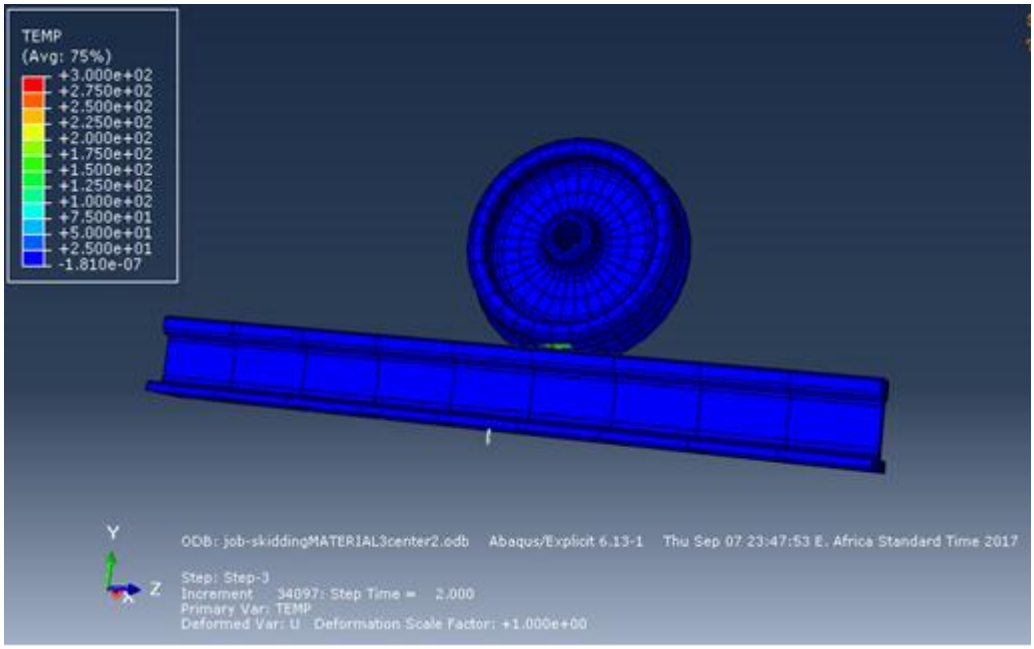

Figure 5.11. Temperature rise of material 2

- The ABAQUS result on the wheel shows that the maximum temperature appears at the central region of the wheel tread where the maximum contact stress on the wheel occurs. The temperature rise of the wheel increases as the wheel slides over the rail. This can be understood from the theory of *Blok's Flash Temperature* that sharp temperature rise takes place at the interface between two rubbing solids upon sliding for a short period.
- The maximum temperature rise is about 325.4^0c, and 300^0c for material-1, and material-2 respectively. A temperature rise beyond 500^0c has a tendency to change microstructural degradation and cause plastic damage on the wheel. Hence material – 1 is more prone to plastic deformation (increase of von-misis stress and plastic strain) for this short running period compared to wheel material – 2.

Graphical representations of results

1. Temperature rise of the two materials

The graphs show the temperature rises of the two materials under a wheel skidding phenomenon.

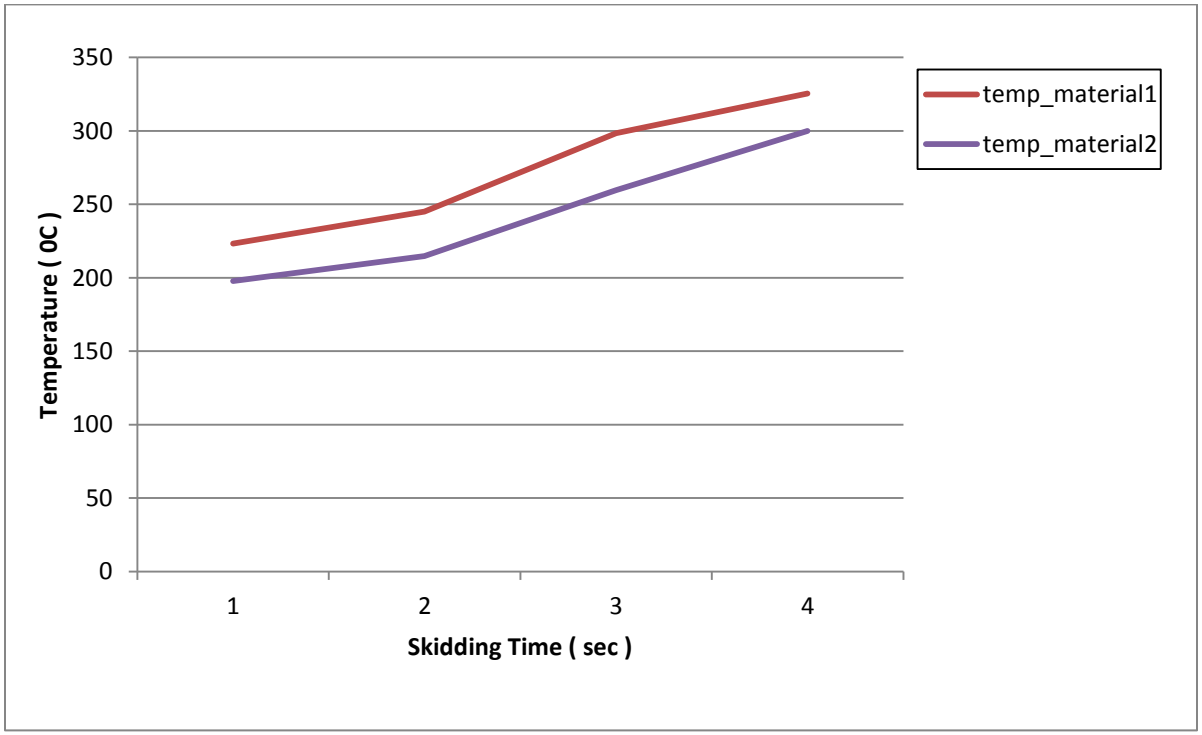

Figure 5.13. Temperature versus skidding tme of the two materials

- The above graph depicts the rise in temperature within the sliding time. It shows that, there is a temperature rise during a wheel skidding phenomenon. This is due to a hard asperity contact created between the two rubbing surface. In this graph the rise in temperature reaches beyond 300^0c for MATERIAL-1. A temperature beyond this limit could change the material property of the wheel that causes deformation and damage. In the contrary the rise in temperature is a bit lowered for MATERIAL -2. This is due to the increased percentage in silicon for MATERIAL-2 since silicon plays the major role in stabilizing surface temperature and high temperature strengthening. It inhibits cementite growth or precipitation and stabilizes pearlite at exposure to high temperature.

2. ***Von misses stress of the two materials***

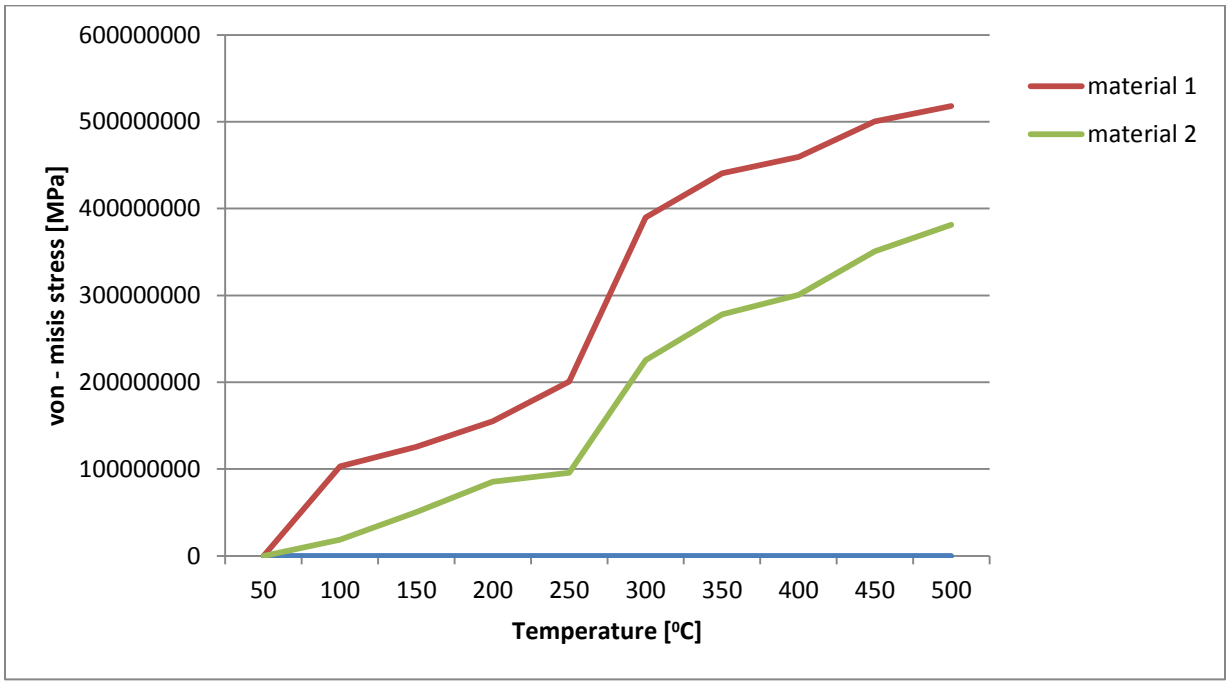

Figure 5.14. Temperature verses Von-mises stress of the two materials

For the same axle- load (11ton) and the same thermal load, the two materials do have different maximum von mises stress. The temperature verses von-mises graph also show that MATERIAL-2 resist thermal stress (temperature rise) compared to MATERIAL - 1. On the graph one can see that von-misis stress increase with the increase of temperature but it also depends on the material property of the wheel. For MATERIAL – 1 the maximum von misis stress is about 517.8 MPa. Similarly for MATERIAL-2 the maximum von-misis is about 381.3 MPa.

3. ***Plastic strain (LE)***

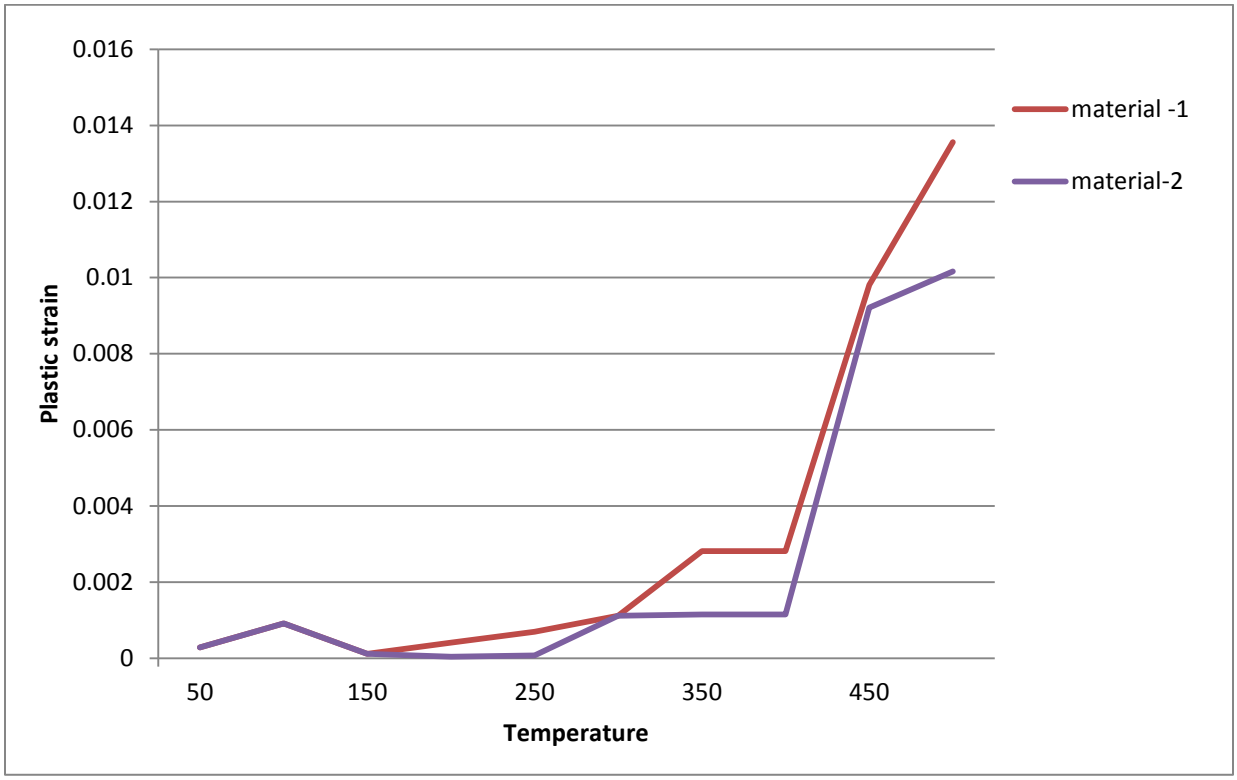

Figure 5.15. Plastic strain verses surface temperature of two materials

The graphical result of the two materials on plastic strain show that plastic strain increases as the temperature of the material rises. But the graph also shows that there is a difference in plastic strain for difference in chemical composition (material property).

0.01356mm and 0.0106mm are plastic strains of material-1 and material-2 respectively. The result shows MATERIAL-2 has the lowest plastic strain compared to MATERIAL - 1. This is because MATERIAL-2 has better alloying content resulting in better resistance for temperature rise.

5.2. Validation of simulation

To validate the results of this paper several literature that are conducted on wheel wear, wheel damage, temperature rise on railway wheel and chemical composition of railway wheel/rail are reviewed. Most of the literatures that are reviewed confirm that wheel plastic deformation is highly dependent on chemical composition and also the rise in temperature aggravates this phenomenon.

The experimental work carried on solid solution strengthening on spalling behavior by the chines scholars indicate that wheel steel with higher silicon and manganese steel (high alloy steel) have lesser plastic damage compared to the other two wheel steels. The scanning electron microscopy (SEM) observation after the twin disc test shows that high silicon and manganese steel have small maretensite zone compared to the other two wheel steels with lesser percentage of alloys silicon and manganese [6].

Their simulation result using ABAQUS software also indicates that plastic deformation is less on high silicon - manganese alloy steel [6].

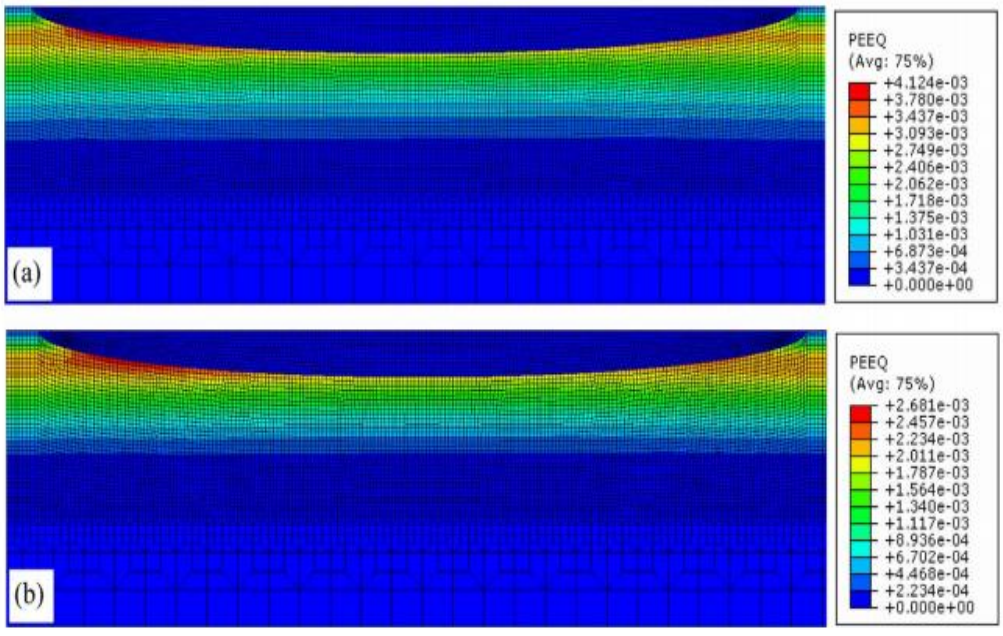

Figure 5.25. Plastic deformation distribution of (a) WEL-ER8 disc and (b) WEL-HiSi disc after the third rolling cycle.

5.3. Discussion

- The ABAQUS result on the wheel shows that the maximum temperature appears at the central region of the wheel tread where the maximum contact stress on the wheel occurs. The temperature rises as the velocity of the train decreases and the sliding of wheel on rail occurs. This can be understood from the theory of *Blok's Flash Temperature* that sharp temperature rise takes place at the interface between two rubbing solids upon sliding for a short period.
- The temperature verses von-mises graph also show that MATERIAL-2 resist thermal stress (temperature rise) compared to MATERIAL - 1. On the graph one can see that von-misis stress increase with the increase of temperature but it also depends on the material property of the wheel. For MATERIAL – 1 the maximum von misis stress is about 517.1MPa. .Similarly for MATERIAL-2 the maximum von-misis is about 381.3 MPa .
- On a plastic strain versus temperature graph, the maximum plastic strain values are 0.0135mm, and 0.010mm for material-1 and material-3 respectively. The result shows MATERIAL-2 has the lowest plastic strain. This is because MATERIAL-2 has better alloying content resulting in better resistance for temperature rise.

CHAPTER 6

CONCLUSION, RECOMMENDATION & FUTURE WORK

Conclusion

- From this short research carried on comparison of wheel material, one can conclude that the strength and temperature resistance property of a wheel material can be enhanced by the increase in important alloys. For a comparison of two wheel materials R6T and R8T (UIC standard), the maximum von – misis stress value are 517.1 MPa, and 381.3 MPa respectively for a corresponding temperature of 325.4^0c, and 300^0c respectively. Similarly the plastic strains are 0.0135mm and 0.0106 for material -1 and material – 2 respectively. These all result of this research show that alloy steel of railway wheel (i.e. a higher weight percentage of silicon and manganese) can resist a wheel plastic deformation and wheel damage such as spalling compared to wheels with a lesser alloy weight percentage.
- The addition of solid solution strengthening elements such as silicon, manganese and other elements increase the wheel resistance for a high temperature rise by decreasing thermal sensitivity.

Recommendation

- The result of this research shows that alloying is the major factor to minimize plastic deformation and wheel damage. Due to temperature rise under wheel operation, railway wheel steel is prone to damage and material degradation. Therefore alloyed steel with more silicon and manganese percentage in a recommended amount is relevant to stabilize temperature rise.
- As the wheel skidding phenomenon occurred on the rail, asperity contact between the wheel and rail will be higher. This contact leads to a higher temperature rise which will leads to plastic deformation and other wheel damage problems. Therefore application of brake force beyond the traction limit of wheel rail contact should be minimized in order to avoid skidding of wheel on rail.

Future work

The following are researches that can be done in the area of wheel deformation;

- Experimental investigation of railway wheel on mitigating plastic deformation and other wheel damage phenomenon.
- Experimental investigation of martensite formation and austenizitation temperature that leads to phase transformation.
- Material development of railway wheel steel based on the study of each alloy and its influence.

Reference

[1]. H. soares, T. zucarelli , M. Vieira, M. Freitas, L. Reis, *Experimental characterization of the mechanical property of railway wheel manufactured using class B material*, XV Portuguese conference on Fracture, Feb. 2016,

[2]. K. Cvetkovski*, J. Ahlström and B. Karlsson, *Thermal softening of fine pearlitic steel and its effect on the fatigue behavior,* Fatigue 2010

[3]. RE.Smallman,I. RHarrisandM.A.Duggan, *Microstructure and Materials Processing, Journal of MaterialsProcessingTechnology63 (1997).*

[4]. S.M. Shariffa,T.K. Palb, G. Padmanabhama, S.V. JoshS.M. ShariffaT.K. Palb, G. Padmanabhama, S.V. Josh, *Influence of chemical composition and prior microstructure on diode laser hardening of railroad steels.* Article, Sep. 2012.

[5]. Johan Ahlstrom, Birger Karlsson, *Microstructural evaluation and interpretation of the mechanically and thermally affected zone under railway wheel flats, May 1999*

[6]. Dongfang Zeng, Liantao Lua,n, Yanhua Gong, Yuanbin Zhang, Jiwang Zhang, *Influence of solid solution strengthening on spalling behavior of railway wheel steel, December 2016*

[7]. *W.*J. Wanga,, R. Lewis, B. Yang, L.C. Guo, Q.Y. Liua,n, M.H. Zhu, *Wear and damage transitions of wheel and rail materials under various contact conditions, June 2016*

[8]. Sinuhe Hernandeza,n, Alejandro Leiro, Manel Rodríguez Ripoll, Esa Vuorinen ,KGustan Sundin, Braham Prakash, *High temperature three-body abrasive wear of 0.25C 1.42Si steel with carbide free bainitic (CFB) and martensitic microstructures, April 2016*

[9]. Dimitrios Nikasn, Johan Ahlström, Amir Malakizadi, *Mechanical properties and fatigue behavior of railway wheel steels as influenced by mechanical and thermal loadings. April 2016*

[10]. A. Mazzù,n, L. Solazzi, M. Lancini, C. Petrogalli, A. Ghidini, M. Faccoli, *An experimental procedure for surface damage assessment in railway wheel and rail steels, August 2015*

[11]. K. Cvetkovskin, J. Ahlstr. *Characterization of plastic deformation and thermal softening of the surface layer of railway passenger wheel treads,* February 2013

[12]. SUHang, PANTao, LILit, YANGCai-Iu, CUIYin-hui,]IHuai-zhon, *Frictional Heat-Induced Phase Transformation on Train Wheel Surface.* JOURNAL OF IRON AND STEEL RESEARCH, INTERNATIONAL, 2008

[13]. T. Zucarelli L. Moreira Filho, H. Soares, M. Vieir , L. Reis, *Experimental characterization of the mechanical properties of railway wheels manufactured using class C material,* September 2016

[14]. Krste Cvetkovski, *Influence of thermal loading on mechanical properties of railway wheel steels,* Department of Materials and Manufacturing Technology CHALMERS UNIVERSITY OF TECHNOLOGY Gothenburg, Sweden 2012

[15]. Katrin Madler, Manfred Bannasch, *Materials used for wheels on Rolling stocks, GERMENY*

[16]. A. Mazzù,n, L. Solazzi, M. Lancini, C. Petrogalli, A. Ghidini, M. Faccoli, *An experimental procedure for surface damage assessment in railway wheel and rail steels,* August 2015

[17]. F. Walther, D. Eifler, *Local cyclic deformation behavior and microstructure of railway wheel materials,* January 2004

[18]. SHENXiao-hui, YANJun ,ZHANGLei, GAOLin, ZHANGJing, *Austenite Grain Size Evolution in Railway Wheel During Multi-Stage Forging Processes, JOURNAL OF IRON AND STEELRESEARCH, INTERNATIONAL.2013,*

[19]. Kazuyuki Handa Yoshisato Kimur , Yoshinao Mishima, *Surface cracks initiation on carbon steel railway wheels under concurrent load of continuous rolling contact and cyclic frictional heat,* June 2009

[20]. K. Cvetkovski, J. Ahlstr¨ Om, *Characterization of plastic deformation and thermal softening of the surface layer of railway passenger wheel treads*. February 2013

[21]. Gen Li, Zhiyuan Hong, Qingzhi Yan, *The influence of microstructure on the rolling contact fatigue of steel for high-speed-train wheel,* October 2015

[22]. Z.K. Fu, H.H. Ding, W.J. Wang, Q.Y. Liu, J. Guo, M.H. Zhu, *Investigation on microstructure and wear characteristic of laser cladding Fe-based alloy on wheel/rail materials,* February 2015

[23]. Y. Zhou, J.F. Peng, Z.P. Luo, B.B. Cao X.S. Jin, M.H. Zhu, *Phase and microstructural evolution in white etching layer of a pearlitic steel during rolling–sliding friction,* May 2016

[24]. H.W. Zhang, S. Ohsaki, S. Mitao, M. Ohnuma, K. Hono, *Microstructural investigation of white etching layer on pearlite steel rail,* January 2006

[25]. Chunlei Zheng, Rui Dan, Fucheng Zhang ,BoLv, Zhigang Yan, Jun Shan Xiaoyan Long, *Effects of retained austenite and hydrogen on the rolling contact fatigue behaviours of carbide-free bainitic steel,* December 2013

[26]. Dongfang Zeng, Liantao Lu, Ning Zhang, Yubin Gong, Jiwang Zhang, *Effect of different strengthening methods on rolling/sliding wear of ferrite–pearlite steel, April 2016*

[27]. Dongfang Zeng, Liantao Lu, Yanhua Gong,,NingZhang ,YubinGong Dongfang Zeng, Liantao Lu , Yanhua Gong ,NingZhang ,YubinGong,*Optimization of strength and toughness of railway wheel steel by alloy design,* December 2015

[28]. T. Kato,, A. Sugeta, E. Nakayama, *Investigation of influence of white layer geometry on spalling property in railway wheel steel,* October 2010

[29]. T. Kato,n, H. Kato, T. Makino, *Effect of elevated temperature on shelling property of railway wheel steel,* April 2016

[30]. Yoshinori OKAGATA*, *Design Technologies for Railway Wheels and Future Prospects,* NIPPON STEEL & SUMITOMO METAL TECHNICAL REPORT No. 105 DECEMBER 2013

[31]. Ajay Kapoor ,The University of Sheffield, *Tribology of Rail Transport,*

[32]. Asitha C. Athukorala, Queensland University of Technology, *Effect of Different Surface Profile on Wear of Rail Steel (AS1085.1) used in Australian heavy-haul railways,*

[33]. Jonas Lundmark, *Rail Grinding and its impact on the wear of Wheels and Rails,*

[34]. Ulf Olofsson and Roger Lewis, *Tribology of the Wheel –Rail Contact*,

[35]. Dr. V.L. Markine, Technische Universiteit Delft, *Wheel/Rail Interface Optimisation,*

[36]. Roger Enblom, *Simulation of Railway Wheel Profile evolution due to Wear,*

[37]. Roger Enblom, *Simulation of Wheel and Rail Profile Evolution Wear Modelling and Validation,*

[38]. Krste Cvetkovski, *Influence of thermal loading on mechanical properties of railway wheel steels,* Gothenburg, Sweden 2012

[39]. Dimitrios Nikas, *Effect of Temperature on Mechanical Properties of Railway Wheel Steels,* Gothenburg, Sweden, 2016

[40]. *William D. Callister, Jr., Materials Science and Engineering,*

[41]. G.K. BURGESS,physicist and P.D. MERICA, Associate physicist, *Some Foreign Specifications for Railway Materials,* Technology papers of the Bureau of Standards, April 20, 1916.

[42]. *Operation and Maintenance Manual for 70% Low Floor Light Rail Vehicle Project of Addis Ababa, Ethiopia*

[43]. K. Knothe, S. Liebelt, *Determination of temperatures for sliding contact with applications for wheel-rail systems*, Berlin, Germany, April 1995

[44]. Dinesh G. Bansal, Jeffrey L. Streator, *Design curves for temperature rise in sliding elliptical contacts*, George W. Woodruff School of Mechanical Engineering, Georgia Institute of Technology, Atlanta, GA 30332, USA, 2009

[45]. Radim Halama, Rostislav Fajkos, Petr Matusekb, Petra Bábkovác, Frantisek Fojtík, Leo Václavek, *Contact defects initiation in railroad wheels – Experience,Experiments and modeling,* October, 2010

[46]. Martin Ertz, Klaus Knothe, *A comparison of analytical and numerical methods for theCalculation of temperatures in wheel/rail contact*, Technische Universität Berlin, Sekr. F5, Marchstr. 12, D-10587 Berlin, Germany, April, 2002.

[47]. Anders Ekberga, Elena Kabo, *Fatigue of railway wheels and rails under rolling contact and thermal loading—an overview*, Department of Applied Mechanics/CHARMEC, Chalmers University of Technology, SE 412 96 Gothenburg, Sweden, October 2004.

[48]. F.D. Fischer, E. Wemer , W.-Y. Yan, *Thermal stresses for frictional contact in wheel-rail systems*, institute of Mechanics. Montanuniversitiit Leoben, A.8700 Leoben. Austria, September 1996.

[49]. Nayan Chandak, Mayank Yede, Prashant Malviya, M.K. Pradhan, *Analysis of railway wheel to study crack initiation due to thermal loading and calculating life cycle*, 5th International Conference of Materials Processing and Characterization (ICMPC 2016), Mechanical Engineering Department, Maulana Azad National Institute of Technology, Bhopal

[50]. Technical Specifications of Vehicles, *China Railway Group (CRECG) Project Manager Office for Light Rail Project of Ethiopia*, July 2013.

[51]. Natnael Tesfamichae, *Identification of the Best Material Combination between Wheel and Rail of Railway Vehicle with Minimum Wear Rate*, May 2015

Appendix

- *Martensite*: Martensite is a non-equilibrium single-phase structure that results from diffusion less transformation of austenite. It may be thought of as a transformation product that is competitive with pearlite and bainite. The martensitic transformation occurs when the quenching rate is rapid enough to prevent carbon diffusion. Any diffusion whatsoever will result in the formation of ferrite and cementite phases. It is a hard and brittle microstructure compared to pearlite and bainite [40].
- *Creep*: the time-dependent and permanent deformation of materials when subjected to a constant load or stress, creep is normally an undesirable phenomenon and is often the limiting factor in the lifetime of a part. It is observed in all materials types; for metals. It becomes important only for temperatures greater than about (absolute melting temperature) [40].

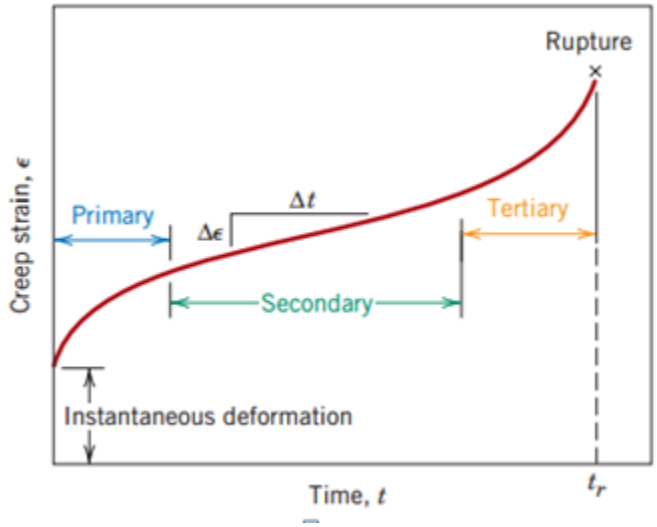

Figure: Typical creep curve of strain versus time at constant stress and constant elevated temperature. The minimum creep rate is the slope of the linear segment in the secondary region. Rupture lifetime is the total time to rupture.

- *Solid solution strengthening:* technique to strengthen and harden metals is alloying with impurity atoms that go into either substitutional or interstitial solid solution. High-purity metals are almost always softer and weaker than alloys composed of the same base metal. Increasing the concentration of the impurity results in an attendant increase in tensile and yield strengths [40].

- *Iron –carbon system Phase diagram*

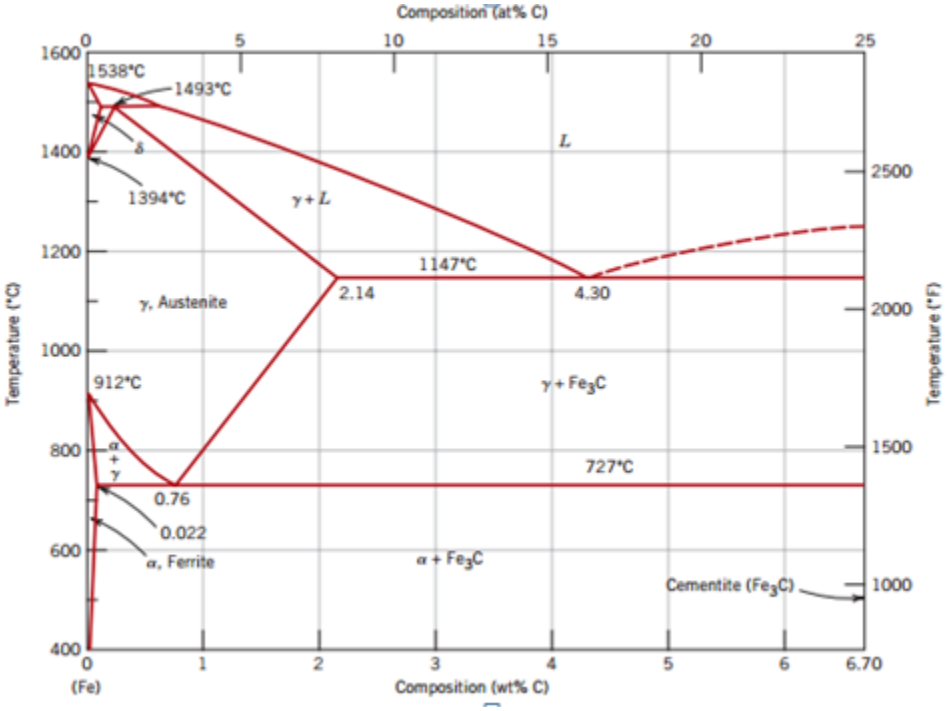

- *Spheroidizing* : Heating the alloy at a temperature just below the eutectoid line A_1 in the region of the phase diagram. If the precursor microstructure contains pearlite, spheroidizing times will ordinarily range between 15 and 25 h.
  - Heating to a temperature just above the eutectoid temperature, and then either cooling very slowly in the furnace, or holding at a temperature just below the eutectoid temperature.
  - Heating and cooling alternately within about of the line.

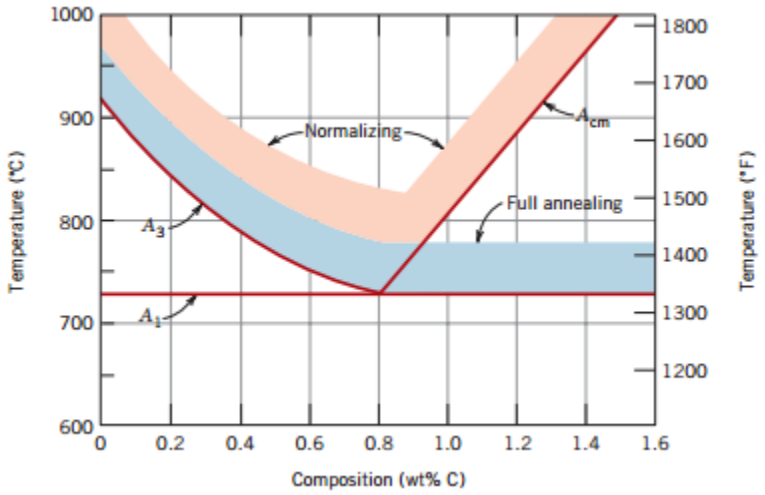

Figure: iron-carbide phase diagram

- *Normalizing:* Steels that have been plastically deformed by, for example, a rolling operation, consist of grains of pearlite (and most likely a proeutectoid phase), which are irregularly shaped and relatively large, but vary substantially in size. An annealing heat treatment called normalizing is used to refine the grains (i.e., to decrease the average grain size) and produce a more uniform and desirable size distribution; fine-grained pearlitic steels are tougher than coarse-grained ones. Normalizing is accomplished by heating at least (55^0c) above the upper critical temperature—that is, above for compositions less than the eutectoid (0.76 wt% C), and above for compositions greater than the eutectoid as represented in the above Figure. After sufficient time has been allowed for the alloy to completely transform to austenite—a procedure termed austenitizing—the treatment is terminated by cooling in air. A normalizing cooling curve is superimposed on the continuous cooling transformation diagram [40]
- *UIC :* International Union of Railways

  The thought of establishing an international organization where all railways could gather together dates back to 23 Nov. 1921 during an international conference in Italy.It was on 3 May 1922 that Geneva international conference was convened and the participating countries encouraged establishment of a permanent rail organization concentrating on rail traffic oriented toward standardization, railway construction and operation improvement.

  UIC include 230 members across all five continents embracing transport operators, infrastructure managers, public transport companies and railways both public and private.

Annex

1. Rail material properties

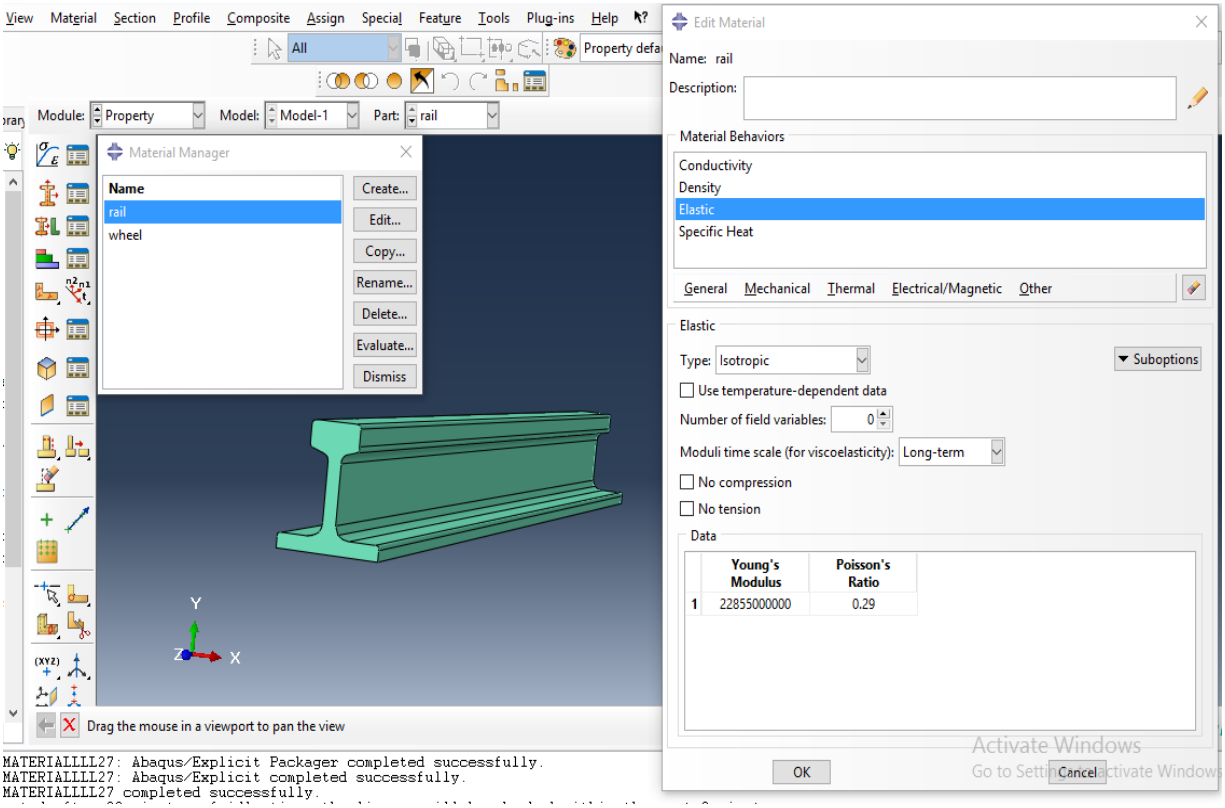

2. Wheel material properties

Material – 1

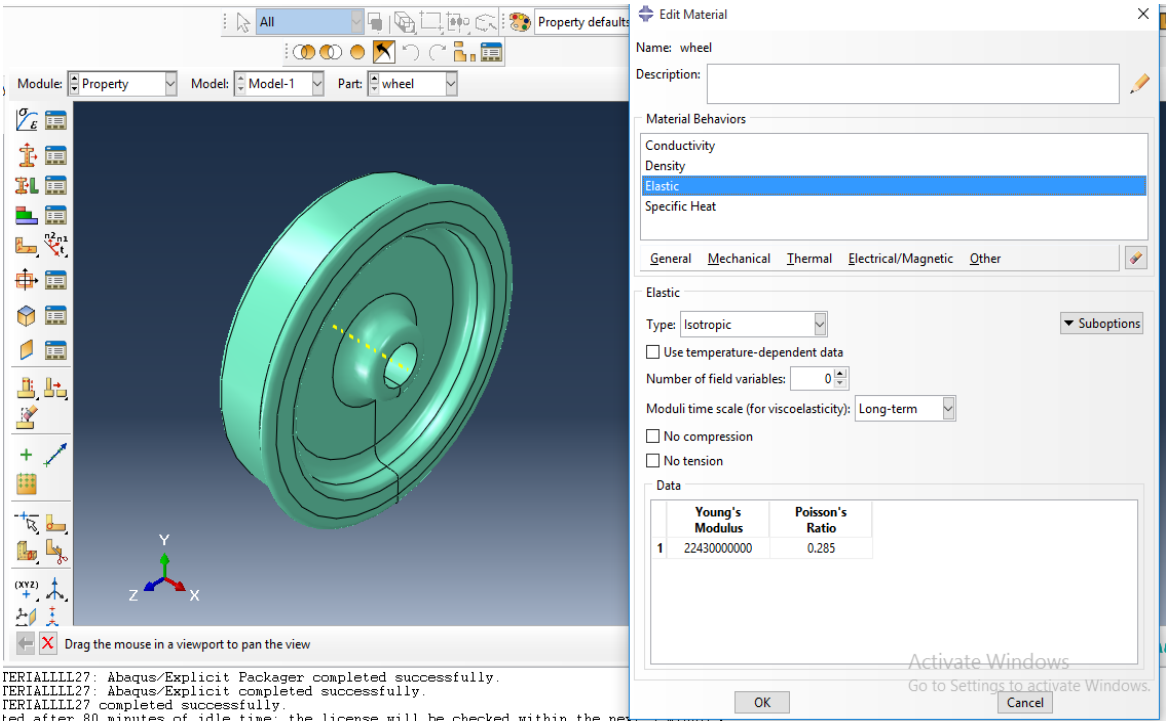

Material – 2

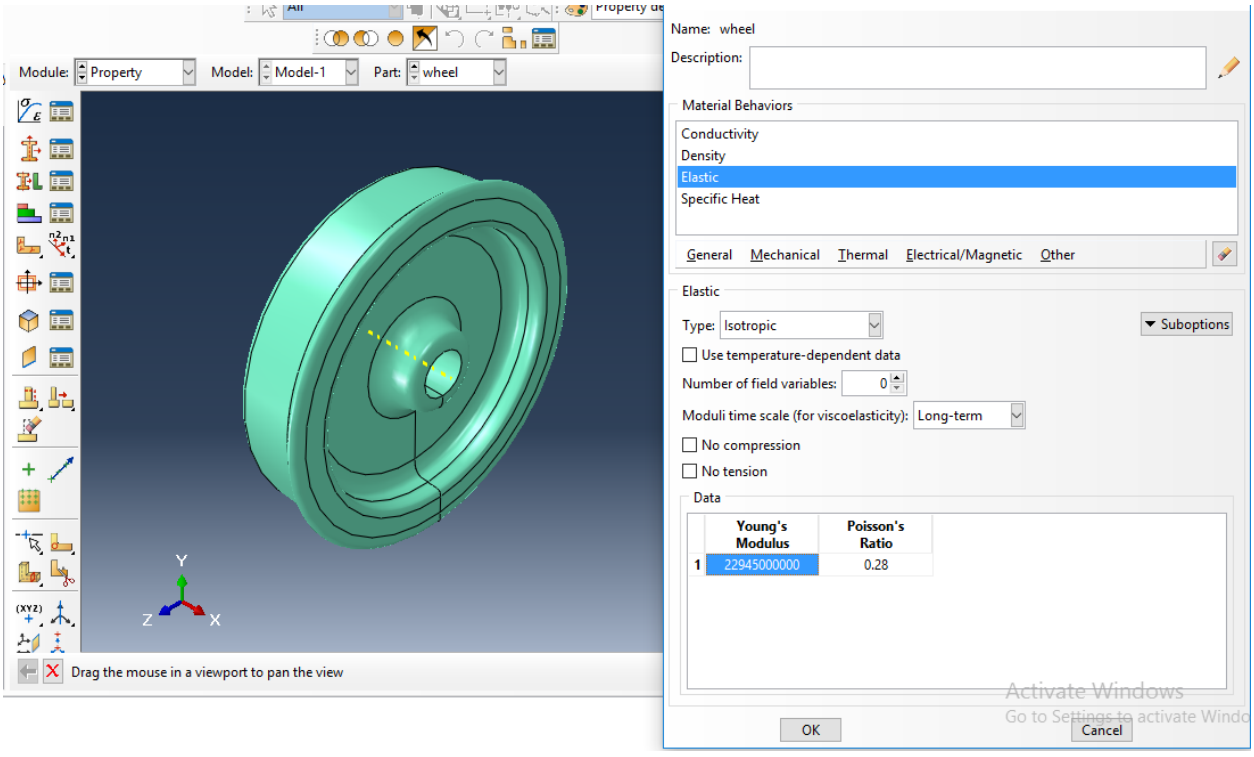

3. Contact condition between the wheel and rail

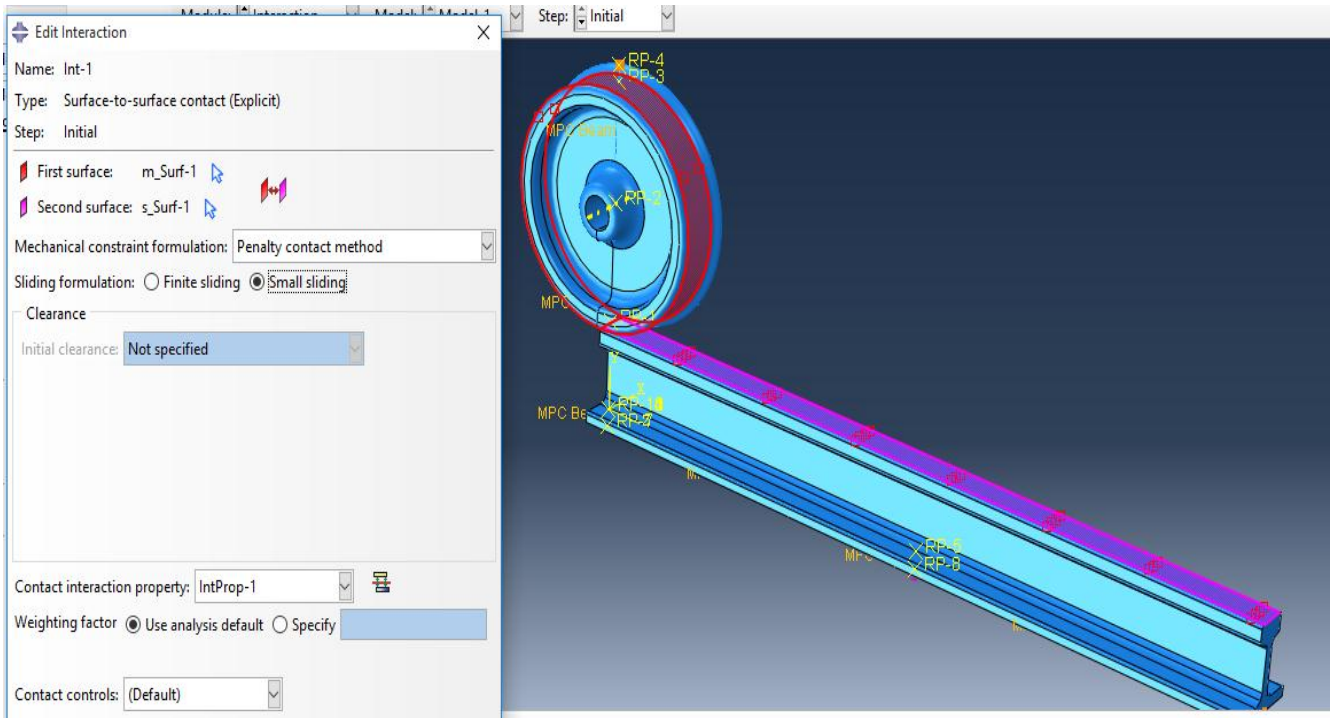

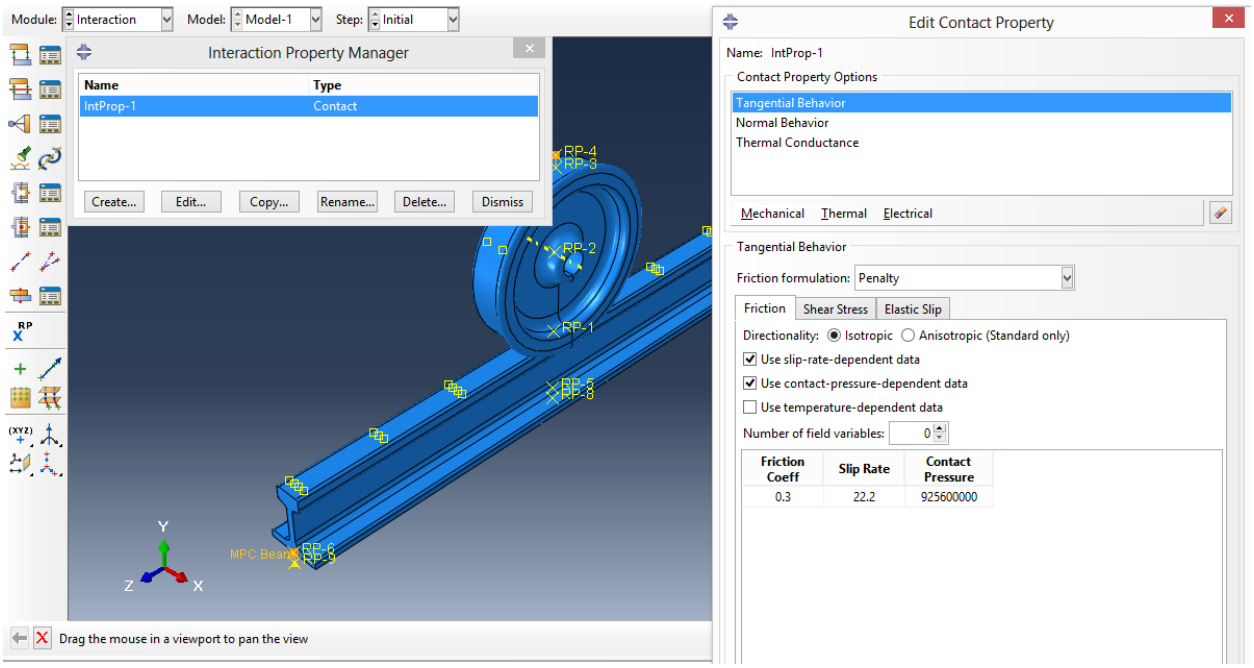

Boundary conditions

Rail

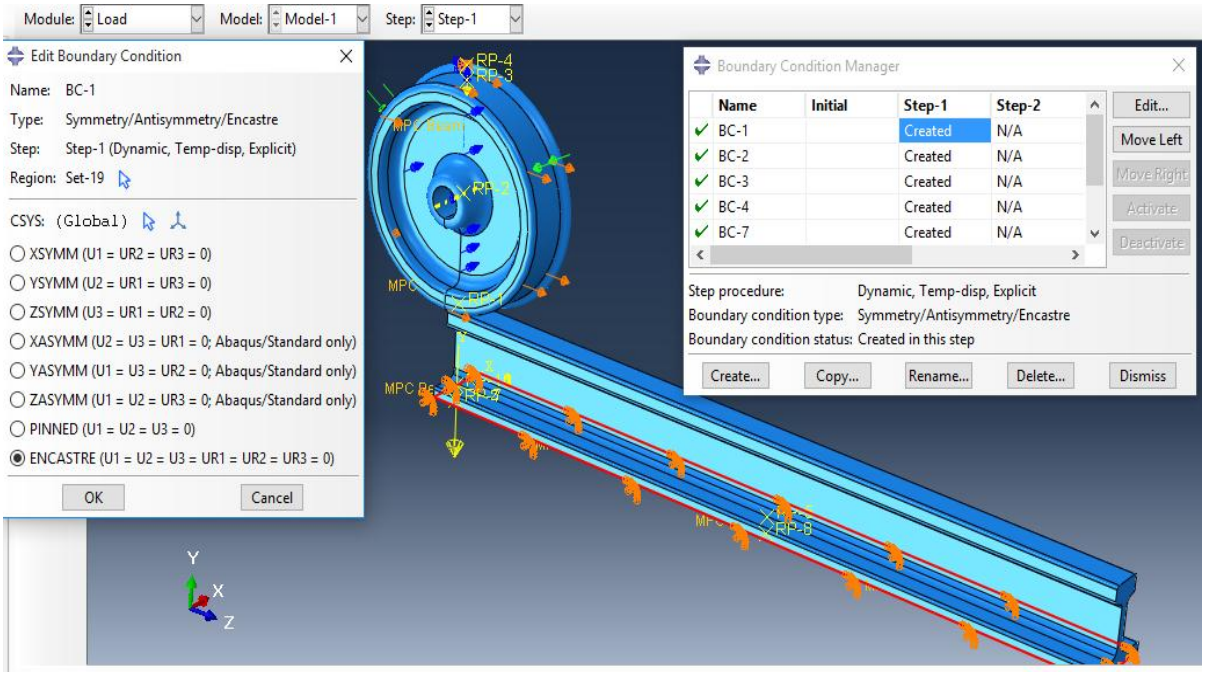

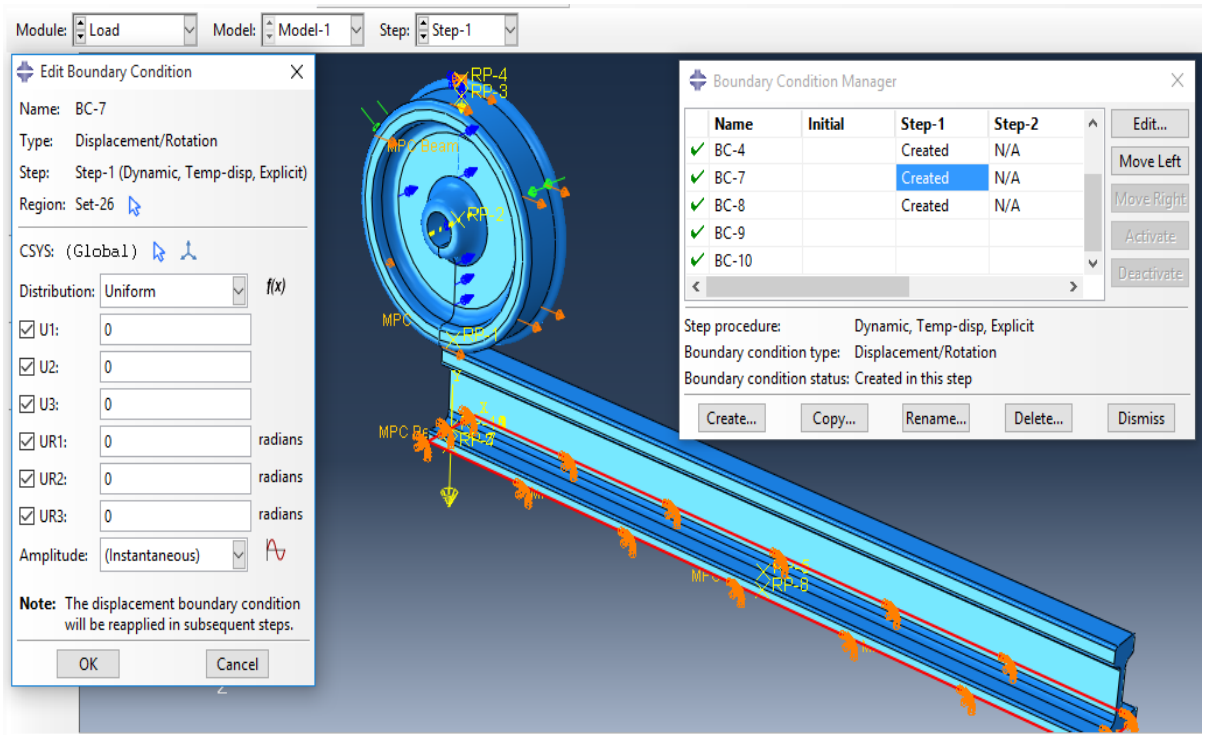

Element

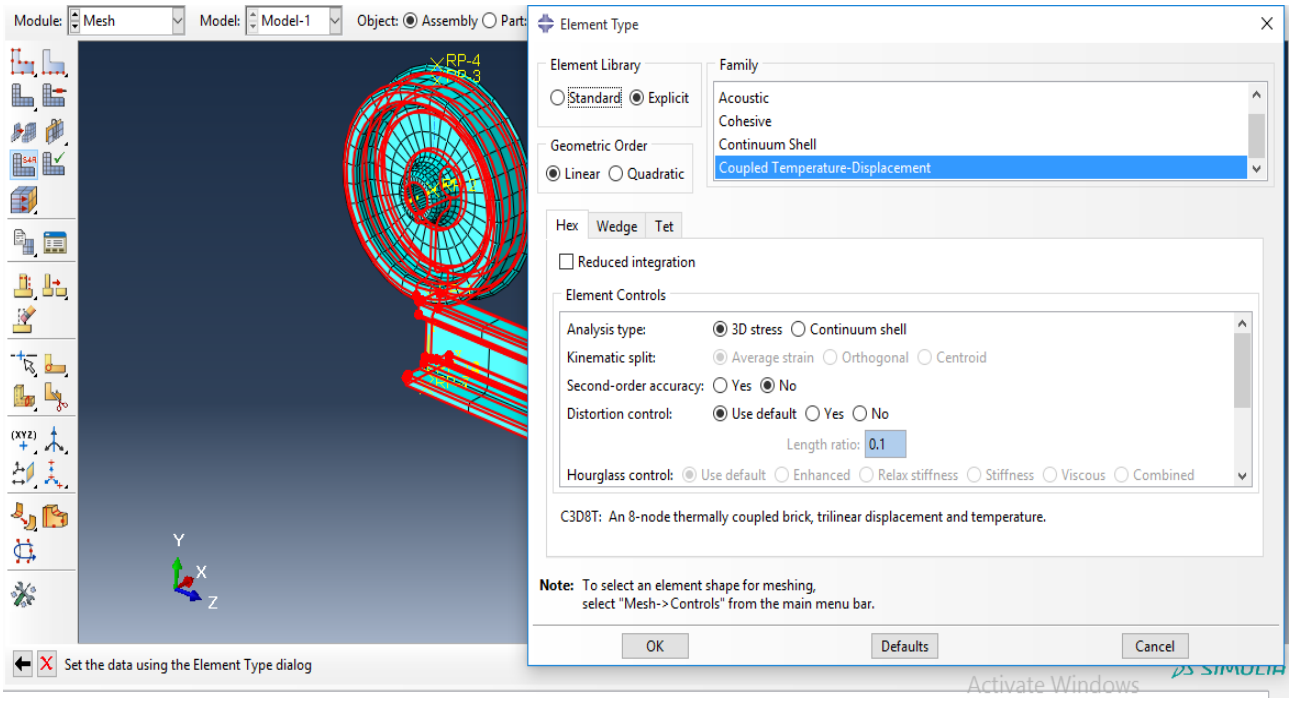
Module: Mesh
Model: Model-1
Object: Assembly Part:
RP-4
RP-3
Element Type
Element Library
Standard Explicit
Geometric Order
Linear Quadratic
Family
Acoustic
Cohesive
Continuum Shell
Coupled Temperature-Displacement
Hex Wedge Tet
Reduced integration
Element Controls
Analysis type: 3D stress Continuum shell
Kinematic split: Average strain Orthogonal Centroid
Second-order accuracy: Yes No
Distortion control: Use default Yes No
Length ratio: 0.1
Hourglass control: Use default Enhanced Relax stiffness Stiffness Viscous Combined
C3D8T: An 8-node thermally coupled brick, trilinear displacement and temperature.
Note: To select an element shape for meshing, select "Mesh->Controls" from the main menu bar.
OK
Defaults
Cancel
Y
X
Z
Set the data using the Element Type dialog
Activate Windows